Maternal effects on early-life gut microbiome maturation in a wild nonhuman primate

Alice Baniel[1,2], Lauren Petrullo[3], Arianne Mercer[4], Laurie Reitsema[5], Sierra Sams[4], Jacinta C. Beehner[3,6], Thore J. Bergman[3,7], Noah Snyder-Mackler[1,2,8,†], Amy Lu[9,†]

AFFILIATIONS

[1] Center for Evolution and Medicine, Arizona State University, Tempe, AZ, 85281, USA

[2] School of Life Sciences, Arizona State University, Tempe, AZ, 85287, USA

[3] Department of Psychology, University of Michigan, Ann Arbor, MI 48109, USA

[4] Department of Psychology, University of Washington, Seattle, WA 98195, USA

[5] Department of Anthropology, University of Georgia, Athens, GA 30602, USA

[6] Department of Anthropology, University of Michigan, Ann Arbor, MI 48109, USA

[7] Department of Ecology and Evolutionary Biology, University of Michigan, Ann Arbor, MI 48109, USA

[8] School for Human Evolution and Social Change, Arizona State University, Tempe, AZ, 85287, USA

[9] Department of Anthropology, Stony Brook University, Stony Brook, NY, 11794, USA

[†]Amy Lu and Noah Snyder-Mackler contributed equally to this work.

Corresponding authors:
Alice Baniel (alice.baniel@gmail.com)
Amy Lu (amy.lu@stonybrook.edu)
Noah Snyder-Mackler (nsnyderm@asu.edu)

ABSTRACT

Early-life gut microbial colonization is an important process shaping host physiology, immunity and long-term health outcomes in humans and other animals. However, our understanding of this dynamic process remains poorly investigated in wild animals, where developmental mechanisms can be better understood within ecological and evolutionary relevant contexts. Using 16s rRNA amplicon sequencing on 525 fecal samples from a large cohort of infant and juvenile geladas (*Theropithecus gelada*), we characterized gut microbiome maturation during the first three years of life and assessed the role of maternal effects in shaping offspring microbiome assembly. Microbial diversity increased rapidly in the first months of life, followed by more gradual changes until weaning. As expected, changes in gut microbiome composition and function with increasing age reflected progressive dietary transitions: in early infancy when infants rely heavily on their mother's milk, microbes that facilitate milk glycans and lactose utilization dominated, while later in development as graminoids are progressively introduced into the diet, microbes that metabolize plant complex polysaccharides became dominant. Furthermore, the microbial community of nursing infants born to first-time (primiparous) mothers was more "milk-oriented" compared to similarly-aged infants born to experienced (multiparous) mothers. Comparisons of matched mother-offspring fecal samples to random dyads did not support vertical transmission as a conduit for these maternal effects, which instead could be explained by slower phenotypic development (and associated slower gut microbiome maturation) in infants born to first-time mothers. Together, our findings highlight the dynamic nature of gut colonization in early life and the role of maternal effects in modulating this trajectory in a wild primate.

INTRODUCTION

The colonization of the gastrointestinal tract begins at birth and develops into a trajectory that can be highly variable between individuals [1–8]. Variation in the source and timing of postnatal microbial colonization influences somatic growth [9–12], neuroendocrine [13,14] and immune physiology [15–17], with health and fitness consequences that can extend across the life course [16,18,19]. In humans, for instance, infants that take antibiotics during the first year of life are more likely to develop allergies, asthma, and inflammatory bowel disease during childhood [20–23]. Germ-free rodent models demonstrate that at least some of these effects are causally related to the microbiome and are long-lasting. For example, germ-free rodents develop structural abnormalities of the gastrointestinal tract [15,24] that translate into immune system dysfunction later in life [25,26], an outcome that can only be partly reversed by introducing microbes during critical periods of development [27,28]. Despite the critical role that early-life gut microbial colonization plays in host development, research thus far has mainly focused on clinical studies in humans [14,22,29–31], complemented by experimental studies on laboratory rodents [32–35] and domestic animals [9,36–39]. Studies of wild animals are needed if we want to understand host-microbiome coevolution within a broader ecological and evolutionary context and without the confounding factors associated with medical interventions (e.g., Cesarean section, antibiotic use, formula feeding) [17,40,41].

The maternal microbiota drives gut microbiome assembly in offspring via vertical transmission of a large number of microbial lineages [42–46]. Vertical transmission is thought to be particularly strong in mammals due to viviparity and extended periods of lactation and post-weaning maternal care [47]. The first important exposure to microbes occurs during birth, when infants are inoculated with maternal vaginal, fecal, and skin microbiota [3,5,8,29,44,48].

67 Postnatally, vertical transmission is primarily accomplished through nursing, with numerous

68 microbes and milk glycans (i.e., oligosaccharides) transmitted through milk that, together,

69 determine the microbial composition of the infant's gut [42,49,50]. While milk microbes directly

70 seed the offspring's gut, milk glycans promote the growth of beneficial microbes, such as

71 *Bifidobacterium* and *Bacteroides*, that in turn break the glycans down into forms usable by the host

72 [51–53]. Although breastmilk is the most obvious route by which vertical transmission takes place

73 [10,49,50,54], studies on humans suggest that the maternal gut microbiome is also a major source

74 of transmitted strains [42,44,55,56]. Maternal gut microbes might be transmitted to offspring via

75 milk, as the gastrointestinal tract is hypothesized to be the major reservoir of microbes colonizing

76 the mammary gland (the enteromammary pathway) [49,57]. Alternatively or additionally, mothers

77 may transmit gut microbes to offspring via preferential body contact [58], a mechanism that

78 suggests vertical transmission can continue in some capacity past weaning [47]. Because maternal

79 microbial taxa are the first to colonize and tend to be better adapted to the gut ecological niche

80 compared to other environmental microbes, they often persist longer in offspring than those

81 acquired from other sources [42,56,59].

82 Recent studies suggest that microbiome-mediated maternal effects are indeed possible. In

83 several mammals, maternal traits, such as parity (i.e., the number of times a mother has given

84 birth), have been associated with differences in the composition of both maternal [39,60] and

85 offspring microbial communities [10,39]. In nonhuman primates (vervet monkeys: *Chlorocebus*

86 *pygerythrus*), infants born to low-parity mothers harbored reduced microbial diversity and a

87 greater abundance of *Bacteroides fragilis [10]*, a bacterium derived from the milk microbiota that

88 is specialized in digesting milk glycans [61,62]. In turn, infants from low-parity females grew

89 faster, suggesting that low-parity mothers may compensate for poor milk production by vertically

90   transmitting milk microbes that could help infants extract more energy from lower milk volumes

91   [10]. Such strategies may be broadly beneficial to dyads in which mothers cannot provide adequate

92   nutritional resources to offspring (e.g., low-ranking mothers) [63,64]. Thus, maternal vertical

93   transmission of microbes may be an important mechanism of phenotypic plasticity during lactation

94   [64,65].

95   Primates are particularly relevant models for understanding postnatal microbiome

96   development and maternal effects because they are closely related to humans, display prolonged

97   lactation periods, and engage in high maternal investment [66,67]. Furthermore, maternal

98   condition (e.g., energetic status) and maternal traits (e.g., dominance rank, social integration

99   parity) are known to influence offspring developmental and long-term fitness outcomes [68–71].

100   Although studies on host-associated microbial communities in wild primates are emerging, many

101   remain limited in scope, hampered by cross-sectional samples and small sample sizes of unweaned

102   infants (particularly in the first few weeks of life), which together prevent longitudinal

103   characterization of gut microbial colonization processes [72–75]. Here, we used dense cross-

104   sectional and longitudinal monitoring to characterize gut microbial colonization during the first

105   three years of life and assess the role of maternal effects in shaping offspring maturation

106   trajectories in wild gelada monkeys (*Theropithecus gelada*). Geladas live in the high-altitude

107   plateaus of Ethiopia and have a specialized graminivorous diet (at times, comprising 90% grass)

108   [76,77], which strongly shapes the composition and function of the adult gut microbiome [78,79].

109   Because geladas live in polygynous reproductive units that range together in larger bands

110   (comprised of 200 or more individuals) [80], we are able to monitor over 50 immatures at any

111   given time, offering an unprecedented sample size to examine gut microbial characteristics during

112   early life in a wild primate. We used 16s rRNA amplicon sequencing on 525 fecal samples from

113 89 immatures to profile changes in gut microbiome diversity, composition, and function during

114 the first three years of life (N=5.9±5.5 samples per individual, range:1-18, **Figure S1**). In our

115 population, geladas reach weaning at approximately 1.5 years of age and become sexually mature

116 around 4.6 years [81]; and maternal characteristics, such as parity and dominance rank, are known

117 to influence inter-individual variation at both of these developmental milestones [Feder et al., in

118 revision; Lu et al., unpublished]. We predicted that early life microbial changes would reflect

119 dietary transitions associated with weaning, as infants transition from milk to a plant-based diet

120 [5,48,82,83]. We also predicted that maternal traits, such as dominance rank and parity would be

121 associated with inter-individual differences in gut microbiome diversity, composition, and

122 function in offspring. More specifically, we predicted that infants born to primiparous and low-

123 ranking mothers would have a microbiome more functionally adapted to digest milk to compensate

124 for poorer maternal energetic allocation during lactation. Lastly, we tested if we could detect

125 evidence of vertical transmission between mother and offspring using fecal-fecal comparisons of

126 mother-infant dyads (with 398 matched fecal samples between mother and offspring collected on

127 the same day throughout development) and if greater vertical transmission in certain females (e.g.,

128 low rank, first-time mothers) could be the conduit for putative maternal effects on offspring's

129 microbiome composition. We expected a stronger signal of vertical transmission in early life

130 [10,42,44,55,56], likely driven by a combination of greater microbial transfer via milk when

131 infants are nursing and are also in more frequent body contact with their mother.

132

133 **RESULTS**

134 *General pattern of gut microbiome maturation in geladas*

135 We characterized the gut microbiome across 525 immature gut microbiome samples, and detected

136 3,784 Amplicon Sequence Variants (ASVs) (mean±SD per sample: 728±261, min-max: 65-1,498)

137   belonging to 19 phyla and 76 families. The gut microbiome composition of immature geladas

138   changed quickly following birth, with an initial phase of taxonomic succession and diversification

139   during the first few months of life, followed by a progressive stabilization of the overall community

140   (**Figures 1A,B**).

141   To characterize broad changes in gut microbial community composition across

142   development, we first focused on patterns of alpha diversity (i.e., the microbial diversity within a

143   sample) and beta diversity (i.e., the overall difference of composition between samples). The

144   Shannon Index of alpha diversity was initially low in early life and increased rapidly with age

145   (GAMM: edf=7.2, $P<2.0 \times 10^{-16}$) (**Figure 1C, Table S1**), converging to adult-like values at 7.3

146   months (nonlinear quadratic plateau model: $R^2=0.62$) (see **Figure S2**, **Table S1** for similar results

147   on alternative alpha diversity metrics). Furthermore, age was one of the strongest predictors of the

148   difference in microbial composition between samples (PERMANOVA based on Aitchison

149   dissimilarity metric of beta diversity: $R^2=0.75$, $P<9.9 \times 10^{-05}$, **Table S2, Figures 1D,E**) and samples

150   clustered tightly by age on the first axis (PC1) of a Principal component analysis of beta diversity

151   (Pearson correlation coefficient between age and PC1=0.62, $P<2.2 \times 10^{-16}$). Compared to alpha

152   diversity, beta diversity reached an adult-like composition later in development, at 17.2 months

153   (nonlinear quadratic plateau model between PC1 and age: $R^2=0.55$; **Figure 1D**), which is

154   approximately the age at which gelada mothers return from lactational amenorrhea and resume

155   reproductive cycles [81]. Other important structuring factors of the immature gut microbiome

156   included infant identity ($R^2=0.24$) and group membership ($R^2=0.05$) (**Table S2**).

157   To assess the compositional maturation of the gut microbiome of immature geladas relative

158   to the maternal gut microbiome across age, we calculated the number of shared ASVs and beta

159   diversity dissimilarity (unweighted and weighted UniFrac) between 398 matched immature-

160   mother pairs of fecal samples collected the same day. As offspring got older, they shared an

161   increasing number of bacteria with their mother (GAMM: effective degree of freedom, edf=4.7,

162   P<2.0x10^{-16}; **Table S3, Figure 1F**) and became more similar to maternal (i.e., adult-like) gut

163   microbiome composition (unweighted UniFrac: edf=4.7, P<2.0x10^{-16}; weighted UniFrac: edf=3.5,

164   P<2.0x10^{-16}; **Table S3, Figure S3**). Convergence with maternal gut occurred at 14.5 months for

165   the number of shared ASVs (nonlinear quadratic plateau model: R^2=0.44; **Figure 1F**) and 14.8-

166   15.5 months for beta diversity dissimilarity (R^2=0.48 for unweighted UniFrac and R^2=0.17 for

167   weighted UniFrac; **Figure S3**).

168   Despite the strong age-related patterns noted above, inter-individual variability in

169   composition (as measured by the minimal pairwise beta diversity dissimilarity value among

170   immature samples, see Methods) was higher among younger infants compared to older juveniles

171   (**Figure 1G**). Some young infants (~3-6 months) in particular had a gut microbiome that were

172   relatively mature (i.e. adult-like) for their age (**Figure 1D**). Such "individuality" in the gut

173   microbiome in early life was likely driven by the presence of rare taxa, since the pattern was

174   stronger using unweighted UniFrac (which does not take into account taxa abundance) as opposed

175   to weighted UniFrac measures of beta diversity (**Figure 1G**).

176

177   ***Taxonomic and functional changes during development***

178   To characterize age-associated changes in microbial composition and function, we used

179   autoregressive integrated moving average (ARIMA) models to identify significant developmental

180   changes in the abundance of each microbial taxa (at the family and genus levels) and each predicted

181   functional pathway (at the metabolic level: KEGG Orthologs, KOs and enzymatic level: Enzyme

182   Commission numbers, EC [84]). We then used hierarchical clustering to group microbial taxa and

183   functional pathways based on similar age-related abundance trajectories. Maturational trajectories

184   fell into one of four distinct clusters at both the taxonomic (**Figure 2, S4; Table S4**) and functional

185   (KOs: **Figure S5-S6**, **Table S5**; EC: **Figure S7**, **Table S6**) levels.

186

187   ***Cluster 1: The early-life microbiome is adapted to process milk***

188   Cluster 1 contained microbes that were abundant during the earliest months of infancy (18

189   families: **Figure 2A, Table S4** and 39 genera: **Figure S4, Table S4**) and are broadly involved in

190   using and fermenting milk sugars (see supplemental results 1 for additional details on cluster 1).

191   These early colonizers comprised bacteria that break down milk glycans (Bacteroidaceae,

192   Bifidobacteriaceae) and lactose (Streptococcaceae, [*Ruminococcus] gnavus group*) and other

193   groups that ferment glycans and lactose into butyrate (Lachnospiraceae: *Lachnoclostridium*,

194   *Blautia*, *Anaerostipes*, and Ruminococcaceae: *Faecalibacterium, Butyricicoccus, Butyricimonas*)

195   or propionate (Veillonellaceae) (**Figures 2B and 3A**). *Bacteroides* appeared to be the main

196   degrader of milk glycans in geladas, representing the most abundant genus in early life (~30% of

197   the gut microbes at 1 month) (**Figure 3A**). One *Bacteroides* ASV − *B. fragilis,* a proficient

198   degrader of milk glycans [61] – was particularly abundant in early life (i.e., with a high loading

199   score on PC1, **Table S7**). By contrast, *Bifidobacterium* − an important milk glycan degrader in

200   humans − was present at extremely low abundance across development (<0.01% at 1 month in

201   geladas vs ~40% in humans [85]) (**Figure 3A**).

202   Functional cluster 1 also reflected the involvement of the gut microbiome in milk

203   utilization and immunity pathways (metabolic cluster 1: **Figures S5-S6, Tables S5** and enzymatic

204   cluster 1: **Figure S7, Table S6**). Young infant gut microbiomes contained high levels of bacterial

205   genes involved in carbohydrate metabolism, notably in the catabolism of fructose, mannose, and

206   galactose (3 abundant milk sugars [86]), and in the conversion of sugars to energy (e.g., via

207   glycolysis/gluconeogenesis, pyruvate metabolism, pentose phosphate pathway) (**Figure 4A**).

208   Similar functional signatures of cluster 1 were also apparent at the enzymatic level, as the gut

209   microbes encoded a specialized enzymatic toolkit (alpha and beta glucosidase, alpha and beta

210   galactosidase, fucosidase, sialidase, beta-hexosaminidase) necessary to cleave complex milk

211   glycans (**Figure S8, Table S6**). *Bacteroides* was the main microbial group encoding those

212   enzymes (**Figure S8**), confirming its central role in milk glycan degradation in geladas.

213   Interestingly, cluster 1 also included several putatively pathogenic genera (**Figure 3B**),

214   including some bacterial species most responsible for enteric infections and diarrheal diseases in

215   human newborns and captive animals (e.g., *Clostridioides difficile*, *Helicobacter macacae*,

216   *Clostridium butyricum, C. perfringens* [87–91]) (**Table S7**). It also included 3 major groups of

217   mucin-degrading bacteria (*Akkermansia*, [*Ruminococcus] gnavus group* and [*Ruminococcus]*

218   *torques*) (**Figure 3C**) that are involved in the development of the intestinal mucosa, a primary line

219   of immune defense [92]. These taxa reflect the importance of the developing immune system at

220   this stage in life. In line with this interpretation, the early life microbial metabolic pathways tended

221   to be more involved in processes related to the host immune system (e.g NOD-like receptor) and

222   nervous system (e.g., glutamatergic synapse pathway) (**Figure 4A, Tables S5**).

223

224   ***Clusters 2 & 3: The weaning transition is accompanied by important gut microbial***

225   ***rearrangements***

226   Around 10 months of age, a small number of microbial taxa (**Figures 2A and S4, Tables S4**) and

227   metabolic pathways (**Figures S5-S6, Tables S5**) peak (cluster 2) or decrease (cluster 3) in

228   abundance. Of these changes, the most notable included peaks in Lactobacillaceae (genus

229   *Lactobacillus*), Prevotellaceae, and Lachnospiraceae (cluster 2, **Figure 2C**). While

230   Lactobacillaceae is a keystone lactic acid bacterial group producing large amounts of lactate from

231   milk sugars, Prevotellaceae and Lachnospiraceae (**Figure 2C**) are fiber-degrading genera. These

232   transient shifts highlight the role of the gut microbiome in digesting both milk and plant items at

233   this age.

234   Taxonomic changes at ten months translated at the functional level into a remodeling of

235   the metabolism of amino acids, with an increase in microbial genes involved in alanine, aspartate,

236   glutamate, cysteine, and methionine metabolism (cluster 2), and a decrease in microbial genes

237   involved in phenylalanine (found in breast milk), glutathione (antioxidant typically enriched in the

238   first weeks of life in humans), and tyrosine metabolism (cluster 3) (**Figure 4B, Tables S5**).

239   Microbial genes involved in sporulation and germination were also more highly expressed (**Figure

240   4B, Table S5**), suggesting some changes in persistence strategy from the spore-forming microbes

241   in the gut.

242

243   ***Cluster 4: The later-life gut microbiome is adapted to a plant-based diet***

244   Cluster 4 was characterized by 22 families (**Figure 2A, Table S4**) and 63 genera (**Figure S4,

245   Table S4**) that increased sharply with age and plateaued in older immatures (from 10 months of

246   age onward), including cellulolytic (Spirochaetaceae, Fibrobacteraceae, *Cellulosilyticum*) and

247   fermentative taxa (Lachnospiraceae, Clostridiales Family XIII, several genera from Prevotellaceae

248   and Ruminococcaceae), as well as RFP12 (**Figure 2D),** which are all commonly found in adult

249   geladas [79]. These taxa are involved in metabolizing complex plant polysaccharides found in

250   graminoid leaves and roots, which comprise the majority of the adult gelada diet.

251   At the functional level (cluster 4, **Figures S5-S6, Tables S5**), the gut of old immatures

252   harbored more bacterial genes involved in energy, amino acid, and lipid metabolism and in the

253   regulation of genetic expression and bacteria growth (nucleotide metabolism, replication and

254   repair, genetic information processing and translation) (**Figure 4C**), a functional profile that is

255   typical of the adult gelada gut [79].

256

257   *Maternal effects on offspring gut microbiome composition and function*

258   We next examined whether inter-individual variability in gut microbiome composition early in life

259   (**Figure 1D,G**) could be explained, in part, by maternal traits, including maternal dominance rank

260   and parity. We ran these analyses using (i) all samples (0-3 years, N=525), but since we predicted

261   that maternal effects on the offspring microbiome would be strongest in early life (when infants

262   are still nursing), we also ran separate analyses only focusing on (ii) young infants (<12 months of

263   age, still relying largely on milk, N=184) and (iii) old immatures (>18 months, relying largely on

264   plants, N=259). Note that we ran separate analyses for each age group because it is not possible to

265   fit an interaction between a smooth term (i.e., age) and covariates (i.e., maternal attributes) in

266   GAMMs.

267   Maternal dominance rank did not influence the alpha or beta diversity (**Tables S1-S2,**

268   **Figure S9**) of immature gut microbiomes, nor did it predict differences in microbial families,

269   genera, or functional pathways (**Tables S8-S10** for (ii) young infants, results not shown for (i) all

270   immatures or for (iii) old immatures). Maternal parity also did not exert a significant influence on

271   the diversity, composition, or relative abundance of taxa in the immature gut microbiome (**Tables**

272   **S1, S2, S8**). However, parity was significantly associated with the relative abundance of several

273   microbial metabolic pathways (**Table S9**) and enzymes (**Table S10**) during the first 12 months of

274   life (results non-significant for (i) all immatures or (iii) old immatures). Namely, infants born to

275   primiparous females had functional profiles more typical of early life (<12 months) and related to

276   milk digestion, both at the metabolic and enzymatic levels. Their gut microbes were more involved

277   in carbohydrate metabolism (e.g., galactose, fructose and mannose metabolism), cellular processes

278   and signaling, and nervous system function (**Figure 5A**); and they harbored a higher abundance

279   of key enzymes that cleave milk glycans (**Figure S10**). By contrast, young infants (<12 months)

280   born to multiparous females had a more functionally "mature" gut microbiome for their age, with

281   higher abundance of later-life microbial pathways such as amino acid metabolism and nucleotide

282   metabolism (**Figure 5B**). To determine why maternal parity had an effect at the functional level

283   but not at the taxonomic level, we examined the bacterial taxa that showed a statistical trend to be

284   more abundant in young infants (<12 months) born to primiparous females (i.e., with p-values<0.1

285   before FDR correction, **Table S9**). Offspring of primiparous mothers indeed tended to harbor a

286   higher abundance of microbial taxa involved in milk digestion (e.g., Lachnospiraceae,

287   Bacteroidaceae, Clostridiaceae 1) (**Figure S11**, see supplemental results 2), which suggests that

288   individual taxa exert small additive effects that were only detected at the functional level.

289

290   ***Mother-to-infant vertical transmission***

291   Previous work on captive primates suggests that the effect of maternal parity on microbial function

292   could be mediated by differences in vertical transmission between multi- and primiparous females,

293   with primiparous females transferring more milk-oriented microbes to their offspring (via the

294   milk) [10]. We tested if we could statistically detect evidence of vertical transmission between

295   mother and offspring using fecal-fecal microbiome comparisons. We used a nonparametric

296   resampling approach to test if mother-offspring pairs of fecal samples were more similar than

297   expected by chance (i.e compared to when we match the immature sample with random adult

298   female samples), as measured by the number of shared ASVs or beta dissimilarity. We predicted

299   that vertical transmission would be strongest in early life (when infants are still nursing), thus we

300   ran analyses using either (i) all samples (0-3 years, N=398 pairs) or focusing on (ii) young infants

301   (<12 months of age, N=136 pairs) and (iii) old immatures (>18 months of age, N=201 pairs)

302   separately. Using all pairs, we found that immatures shared 3.4% more ASVs (observed

303   value=355, random value=343, P<1.0x10^{-3}) and were 1.8% more similar compositionally

304   (unweighted UniFrac dissimilarity: observed=0.55, random=0.56, P=1.0x10^{-3}) to their own

305   mother than with random adult females of the population (**Table S11**), potentially indicative of

306   vertical transmission. However, unexpectedly, this signal was weaker and non-significant in the

307   youngest infants (0-12 months: number of shared ASVs: observed=251, random=245, P=0.09 and

308   unweighted UniFrac dissimilarity: observed=0.67, random=0.67, P=0.26; **Figures 5C and S12,**

309   **Table S11**), and was strongest and significant in older juveniles (>18 months: number of shared

310   ASVs: observed=412, random=398, P=2.0x10^{-3} and unweighted UniFrac dissimilarity: observed

311   value=0.49, random value=0.50, P=1.0x10^{-3}; **Figures 5C and S12, Table S11**). The finding of

312   greater vertical transmission after, rather than before, nursing cessation suggests that these mother-

313   offspring similarities were mostly mediated by non-nursing interactions and that milk vertical

314   transmission may not be adequately captured by comparing infant and maternal fecal microbiomes.

315   Moreover, the ASVs shared between mother-infant pairs in the first 12 months of life were

316   not the same ASVs found abundant in early-life (i.e., ASVs with a negative score on PC1) and

317   therefore not related to nursing (**Figure 5D, Table S12**). For example, *Bacteroides fragilis* is found

318   in 49% of infants <12 months but is only shared in 9% of mother-infant pairs. Instead, the most

319   commonly shared ASVs among mother-infant pairs between 0-12 months tended to be ASVs

320   characterizing later life (i.e., with positive scores on PC1), characteristic of older offspring and of

321   adult females (**Figure 5D, Table S12**). Thus, mother-infant pairs share more bacteria and have

322   more similar gut microbial community than expected by chance, but this shared community

323   belongs to the typical adult microbiome of geladas, and is not specific to microbes functionally

324   beneficial to processing milk during the early developmental period.

325   Since infants of primiparous females possessed more milk-oriented microbes (i.e., far from

326   adult-like microbes), we also found that they shared fewer ASVs (ß=-74.5, P=0.01) and were more

327   dissimilar to their mother (unweighted UniFrac: ß=0.07, P=0.03) in the first 12 months of life than

328   infants born to multiparous females (**Figure 5E, Table S3**). However, this effect of greater

329   dissimilarity in primiparous-infant dyads disappeared later in life (>18 months of age) when the

330   effect of maternal parity was no longer detected (number of shared ASVs: ß=11.0, P=0.46,

331   unweighted UniFrac: ß=-3.5x10^{-3}, P=0.81) (**Figure 5E, Table S3**). This result shows that the

332   effect of maternal parity on the offspring gut microbiome in the first 12 months of life is not

333   mediated by stronger vertical transmission of milk-oriented microbes when using fecal-fecal

334   comparisons.

335

336   **DISCUSSION**

337   We provide a detailed description of the compositional assemblage and functional development of

338   the infant gut microbiome in a nonhuman primate during the first three years of life. As expected,

339   age was the strongest structuring factor of the diversity, composition, and function of the gut

340   microbiome. Most microbial taxa had clear age-related trajectories and could be grouped into four

341   main clusters that reflected progressive dietary transitions associated with weaning. In addition,

342   our data show that maternal effects were an important factor modulating offspring gut microbiome

343   both during nursing and after weaning.

344   The broad dynamic of microbial colonization in geladas presents many similarities with

345   previous reports on humans [2,5,8] and other mammals ([10,37,73], but see[74]). We observed a

346 low initial number of microbes and a rapid increase in microbial diversity in the first seven months

347 of life, followed by more gradual changes in microbial composition until weaning (~17 months).

348 The fact that maximal microbial diversity was attained by the time infants reached 7 months, while

349 the microbial community continued to evolve until weaning, suggests that numerous events of

350 lineage extinction and *de novo* colonization continue to take place in the gelada gut until weaning.

351 Similar to humans [5,42,93], it is the cessation of nursing rather than just the introduction of solid

352 foods (which usually starts as early as the first few weeks after birth in geladas) that really drives

353 the maturation of the developing gut microbiome to an adult-like composition. Indeed, weaning

354 marks two important transitions that can have dramatic effects on the maturing gut microbiome.

355 First, as milk is replaced by solid foods, the nutrient sources for host and microbes both change,

356 altering the types of microbes that are likely to flourish. Second, weaning is accompanied by the

357 loss of maternal-origin immunologic factors and milk-derived microbes [94], both of which can

358 further alter the microbiome through processes of selective seeding. Shifts in gut microbiome

359 composition and function closely followed progressive dietary transitions: gut bacteria that

360 facilitate milk glycans and lactose utilization were dominant in the gelada microbiome during early

361 infancy, while cellulolytic and fibrolytic bacteria that metabolize plant complex polysaccharides

362 were dominant later in development as graminoids were progressively introduced in the diet [76].

363 Many of the early life colonizers were similar to those found in humans, such as *Bacteroides*,

364 *Streptococcus*, *Faecalibacterium*, Lachnospiraceae, *Blautia*, *Clostridium*, *Veillonea*, *Escherichia-*

365 *Shigella*, and Pasteurellaceae [48,82,95] which perhaps suggest a set of universal mammalian or

366 primate infant microbial taxa. These early-life microbes work as a metabolic network that relies

367 on cross-feeding between primary degraders (e.g., lactose-degraders such as *Streptococcus*) and

368 secondary fermenters (e.g., lactate-utilizers such as *Veillonea*) to convert milk sugars into energy

369   [96]. The functional enrichment in carbohydrate metabolism and fermentative pathways found in

370   gelada infants is also typically observed in human newborns [2,5,55,97].

371   *Bacteroides*, and in particular *B. fragilis [61,98]*, appear to be the primary microbial taxa

372   involved in milk glycan degradation in geladas, as evidenced by their high abundance in early-life

373   and the fact that they encode the enzymatic toolkits necessary to cleave complex milk glycans

374   (e.g., fucosidase, sialidase, beta-galactosidase). These bacterial enzymes are critical for host

375   nutrition, as mammalian hosts are unable to produce them and therefore cannot utilize milk glycans

376   independently of gut bacteria [82]. In humans, this function is largely met by *Bifidobacterium*, a

377   taxa commonly found in high abundance in breastfed humans that also breaks down milk glycans

378   [8,48,99,100]; however this taxon was almost entirely absent in young geladas. In fact, variation

379   in the dominance of *Bifidobacterium* and *Bacteroides* appears the norm at both the species and

380   population level: several studies in mammals [10,37,72,101] and in some human populations

381   [3,85,95,97,102] have noticed the absence of *Bifidobacterium* but abundance of *Bacteroides* in

382   most or at least some nursing infants. *Bifidobacterium* and *Bacteroides* have different glycan-use

383   profiles [61,62,97] linked to species and population differences in milk composition, particularly

384   the structure and the relative abundance of different milk glycans [103–105].

385   The early-life microbiome of geladas was also characterized by a high number of

386   potentially pathogenic bacteria known to cause enteric infection in human newborns and captive

387   animals (*Clostridioides*, *Helicobacter*, *Clostridium*) [87–91] and several bacterial groups involved

388   in the activation of the host immune system such as butyrate-producing (*Blautia*,

389   *Faecalibacterium, Butyricicoccus, Butyricimonas*) and mucin-degrading bacteria (*Akkermansia*,

390   *Ruminococcus gnavus* and *R. torques*). Collectively, this microbial profile suggests that immune

391   function is a priority for gelada infants. Butyrate plays a key role in the maintenance of gut integrity

392   [106,107] and protection against enteric infection [108]. This microbial metabolite is also an

393   important immunoregulator via its action on intestinal macrophages [109,110]. Mucolytic bacteria

394   play an essential role in mucus turnover [111] and contribute to an essential immune barrier

395   protecting the underlying epithelium from luminal pathogens [111] and are thus strongly involved

396   in immunity in early life. *Bacteroides* are also likely involved in regulation of intestinal immunity

397   in early life [112,113]. *Bacteroides fragilis* in particular is directly involved in the maturation of

398   the immune system by directing the production of regulatory T cells and ensuring a balance

399   between Th1 and Th2 immunologic response [114–117]. Functional analyses revealed that the gut

400   microbes were more strongly involved in host immunity during the nursing period, highlighting

401   that microbial colonization plays an important role in priming of the host immune system in

402   geladas.

403   We detected important compositional and functional signatures of microbial rearrangement

404   around 10 months of age (i.e., 5-7 months before nursing cessation). *Bacteroides* decrease

405   substantially in the gelada gut microbiome, while two other taxa, *Lactobacillus* and *Prevotella,*

406   increase in abundance. *Lactobacillus* is a lactic acid bacterium that consumes lactose [118,119].

407   Its rise in abundance around the weaning transition indicates an increase in lactose availability in

408   the colon, likely due to the loss of endogenous lactase of infants in the upper gut [120]. *Prevotella*

409   is a keystone fiber-degrading bacterium typically enriched in individuals with a plant-based diet.

410   In two other mammalian species (vervet monkeys: [10] and northern elephant seals (*Mirounga*

411   *angustirostris*): [72]), *Prevotella* also increased in abundance during the weaning transition. The

412   abundance of *Bacteroides* and *Prevotella* are generally inversely correlated in the gut, due to the

413   trade-off between saccharolytic and proteolytic fermentation [121]. Thus, the growth of *Prevotella*

414   closer to weaning might be related to the decrease in milk degrading bacteria (i.e., *Bacteroides*)

415   and could be a good indicator of the transition from milk to solid food consumption in mammals

416   [10]. These taxonomic changes were also accompanied by important functional changes in the

417   metabolism of amino acids, vitamins, and cofactors, setting up the microbial activity characteristic

418   of the adult gut.

419   　　　Finally, our results highlight that early-life gut microbiome composition and functionality

420   can be influenced by maternal effects, both during the nursing period, but also after weaning.

421   During the first 12 months of life, we found that infants of primiparous mothers harbored more

422   bacteria that were functionally relevant for processing milk sugars, which parallel recent findings

423   in vervet monkeys [10]. The authors in that study hypothesized that infants of primiparous mothers

424   may compensate for poor maternal investment by seeding more milk-oriented microbes that help

425   infants extract more energy from milk [10]. In support of this, *B fragilis* was more abundant in the

426   milk of low-parity vervet females, which resulted in higher abundance of milk-oriented microbes

427   in the infant gut, which in turn promoted faster growth in low-parity infants [10]. In our study,

428   vertical transmission – as assessed by fecal-fecal comparison of maternal and offspring

429   communities – was not identified as the mechanism generating such a parity effect. First, we did

430   not find evidence of vertical transmission in the first 12 months of life (infants and mothers did

431   not share more ASVs than expected by chance during nursing). Second, the microbes that *were*

432   shared by mother-offspring pairs were associated with processing grass rather than early life

433   functions such as processing milk glycans or sugars. Third, infants from primiparous females

434   actually shared fewer microbes with their mother than infants from multiparous females (since the

435   detected shared microbes are later-life microbes). This result suggests that vertical transmission of

436   early colonizers/milk-oriented microbes might be more strongly mediated by the direct transfer of

437   milk microbiota in geladas [10,49,50,54] and, in contrast to reports in humans [42,44,55,56], not

438   easily detected using fecal-fecal comparisons between infants and their mothers. In vervets, for

439   instance, infants aged 2-5 days shared more bacterial strains with their mother's milk than with

440   their mother's gut [10]. This parity effect could nonetheless result from host filtering processes

441   coming from the offspring themselves [56]. Maternal microbiomes might be similar across parity

442   status, but offspring of primiparous females might preferentially seed milk-oriented microbes from

443   milk in response to poorer maternal energetic allocation. In the absence of milk samples, evidence

444   for such mechanisms remains unclear in geladas.

445   Alternatively, the effect of maternal parity could reflect a faster pace of gut microbiome

446   maturation for offspring born to multiparous mothers. The pattern of vertical transmission might

447   be similar between primiparous and multiparous females, but offspring of multiparous females

448   might share more microbes with their mother during the first 12 months of life because they are

449   more mature for age (and because we only capture vertical transmission of grass-processing

450   microbes). This interpretation is supported by the evidence that multiparous mothers wean their

451   offspring about 5 months earlier than primiparous females in geladas (in our studied cohort and in

452   absence of takeover: multiparous=17.1 months, primiparous=21.9 months). The greater similarity

453   between multiparous mothers and their infants is thus more likely to be generated by accelerated

454   gut microbiome development, suggesting that these infants are undergoing the weaning transition

455   at a faster pace than their peers. Infants from multiparous females could be eating solid grass,

456   gaining physical independence, and becoming socially integrated earlier than their peermates, all

457   of which could explain greater microbial resemblance to mothers (and other adults). Behavioral

458   and development data, such as infant growth, are needed to investigate this hypothesis of

459   accelerated development and their consequences on offspring phenotype.

460   Somewhat surprisingly, we did find that immature gut microbiomes were more similar to

461   maternal gut microbiomes than expected by chance after weaning regardless of the parity status of

462   the mother. Such an effect has been previously documented in wild red squirrels (*Tamiasciurus*

463   *hudsonicus*) [122] and chimpanzees (*Pan troglodytes*) ([74] but see [123]). Host genetics, or

464   socially transmitted microbes, may facilitate maternal-offspring gut microbiome similarities

465   beyond the early postnatal period [47]. A recent study in yellow baboons (*Papio cynocephalus*)

466   found that the gut microbiome, including both abundant and rare taxa, is highly heritable [124]

467   suggesting that the convergence of the gut microbiota between mother and offspring in geladas

468   could be due shared genes. Alternatively, or additionally, the higher similarity in later life could

469   be generated by high frequency of social contacts between mothers and offspring that extend past

470   weaning. Primate mothers and offspring form preferential social bonds long after weaning,

471   relationships that are characterized by a high degree of proximity, physical contact and grooming,

472   and are likely to represent an enduring source of maternal microbial inoculation for offspring

473   [58,125]. Further work is needed to understand the relative importance of these mechanisms in

474   explaining mother-infant similarity during juvenility.

475

476   ***Conclusion***

477   Our results highlight that early-life gut microbiome composition and function can be influenced

478   by maternal effects, both during nursing as well as after weaning. Maternal parity in particular was

479   associated with the functional maturation of the microbiome in offspring, likely reflecting faster

480   developmental pace of infants born to reproductively experienced mothers. As infants age and are

481   weaned, they converge toward an adult-like gut microbiome that is more similar to the maternal

482   gut microbiome than expected by chance. The long-term consequences of such microbially-

483   mediated maternal effects remain unknown but could potentially influence phenotypic outcomes

484   such as growth and immune function. Our work also emphasizes that early life vertical

485   transmission, mediated in large part by milk transfer, may not be detected using fecal-fecal

486   comparisons of maternal and infant communities and would ideally require data on the milk

487   microbiome whenever possible.

488

489   **MATERIAL & METHODS**

490   ***Study population and study site***

491   The data for this study were collected between Jan 2015 and Jan 2019 from a population of wild

492   geladas living in the Simien Mountains National Park in northern Ethiopia (13°15′N, 38°00'E).

493   Geladas live in multi-level societies, where several reproductive units (comprising a leader male,

494   several adult females, their offspring, and occasionally 1–2 follower males) aggregate together

495   during the day to forage and sleep together forming a "band", sharing a homerange [80]. Since Jan

496   2006, the Simien Mountains Gelada Research Project (SMGRP) has collected behavioral,

497   demographic, and genetic data on a near-daily basis from over 600 individuals living in 2 separate

498   bands of the area. All gelada subjects were habituated to human observers on foot and were

499   individually recognizable. Data were derived from 89 infants and juveniles aged between 0-3 years

500   old and 83 adult females living in 23 different reproductive units. The date of birth of each infant

501   was known within a few days' accuracy. The reproductive state of each adult female was

502   monitored daily and recorded as cycling (as indicated by the presence of sex skin swellings on the

503   neck, chest, and perineum), lactating (if she had a nursing infant), or pregnant (the date of

504   conception was inferred by removing 183 days from the date of birth of subsequent offspring)

505   [81]. Records of female reproductive history were used to assign maternal parity status for each

506   infant (first-time mother: primiparous or multi-time mother: multiparous) and to establish the date

507   at which the mother resumed cycling following the infant's birth, which we used to estimate the

508   approximate age at weaning for each infant. For 8 infants, age at weaning began on the date of

509   maternal death.

510

511   ***Fecal sample collection***

512   Fecal samples (N=525; 303 females, 222 male samples) from 89 immature geladas (i.e., infants

513   and juveniles sampled pre-reproductive maturity; female: N=51; male: N=38,

514   mean±SD=5.90±5.53 samples per individual, range=1-18) were collected opportunistically from

515   2015-2016, and then regularly from 2017 to 2018) during the development using targeted protocols

516   (**Figure S1**). These samples come from individuals residing in 17 different reproductive units

517   (mean±SD= 5.65±4.44 number of individuals sampled per unit, range=1-17). For a subset of

518   immature samples (N=398 samples from 61 infants), we also collected a matched fecal sample

519   from the mother (N=398 samples from 44 mothers) on the same day or on the following day of the

520   infant sample collection. Fecal samples of known adult females in all reproductive states were also

521   routinely collected (N=222 samples from 79 females) and were used to generate a random

522   distribution of gut microbiome composition similarity between females of the population and

523   immatures. Immediately upon defecation, approximately 1.5 g of feces was collected in 3 ml of

524   RNA later [126] stored at room temperature for up to 2 months, and subsequently shipped to the

525   University of Washington (UW). At UW, samples were stored at -80°C until the sequencing

526   libraries were prepared.

527

528   ***Maternal dominance ranks***

529 Female dominance ranks were established using *ad libitum* and focal observations of agonistic

530 interactions between all adult females belonging to the same unit with an Elo-rating procedure

531 [127] implemented in the R package EloRating [128]. Agonistic interactions included physical

532 aggression (hit, bite), chase, threats (vocal threats, non-vocal gestures), approach-avoid

533 interactions (displacements) and submissive behaviors (fear bark, crouch, grimace). In geladas,

534 agonistic interactions usually consist of a sequence of several behaviors in a row emitted and

535 received by both parties. Since it can be difficult to establish the winner of each agonistic sequence,

536 we consider each behavior of a sequence as a separate event and assign the winner and loser based

537 on the directionality of the behavior. We obtained a daily Elo-score that we then averaged per

538 month. Since Elo-scores can be sensitive to differences in sampling effort, we then converted this

539 monthly Elo-rank into a monthly proportional rank and controlling for female group size

540 (0=lowest-ranking females and 1= highest ranking female). In the analyses, we used maternal

541 dominance rank during the month of the infant's birth since we expect microbially-mediated

542 maternal effects to be the strongest in the postnatal period (during nursing). However, we also

543 investigated maternal rank during pregnancy and at the date of immature sample collection, which

544 led to similar results (not reported here).

545

546 **Environmental data**

547 The study area is located at 3200 m above sea level and is characterized as an Afroalpine grassland

548 ecosystem, consisting of grassland plateaus, scrublands, and Ericaceous forests [129]. The climate

549 in the Simien Mountains National Park exhibits marked inter- and intra-annual fluctuation in

550 rainfall and temperature and can be broadly divided into 3 distinct seasons : a cold-dry season (Oct

551 to Jan), a hot-dry season (Feb to May) and a cold-wet season (Jun to Sep) [130]. Fecal samples of

552   immatures and adult females were collected across the year, with roughly equal coverage across

553   seasons (406 in cold-dry, 426 in cold-wet and 313 in hot-dry season). Daily cumulative rainfall

554   and minimum and maximum temperature are recorded on a near-daily basis by the SMGRP.

555   Geladas are graminivorous, with up to 90% of their diet composed of graminoids [76]. They eat

556   primarily graminoid leaves (i.e., grasses and sedges) all year long, but increase substantially their

557   consumption of underground storage organs (rhizome, corms, roots) in the dry season, as above-

558   ground graminoid leaves become less abundant [76]. A previous study established that the gut

559   microbiome composition of adults shifts in response to environmental variation, in particular with

560   cumulative rainfall which is a good proxy of diet. [79]. Thus, in all models we controlled the total

561   cumulative rainfall over the 30 days prior to the date of fecal sample collection (as a proxy for

562   grass availability) and the average minimum daily temperatures in the 30 days preceding the date

563   of sample collection (as a proxy of thermoregulatory constraints).

564

565   *16S rRNA gene sequencing*

566   We performed 16S rRNA gene amplicon sequencing on the immature and female fecal samples to

567   establish gut microbial composition. We first extracted microbial DNA using Qiagen's

568   PowerLyzer PowerSoil DNA Isolation kit (Qiagen #12855) following standard protocols. We then

569   amplified the hypervariable V4 region of the 16S rRNA gene using PCR primer set 515F and 806R

570   from The Human Microbiome Project and a dual-indexing approach [131]. Details of the

571   amplification protocol can be found in [79] (see also: https://smack-lab.com/protocols/). The

572   libraries were then pooled in roughly equimolar amounts (each with their own unique indexing

573   primer combination), spiked with 10% PhiX to increase library complexity, and sequenced

574 together on a single Illumina NovaSeq 6000 SP 250 bp paired-end sequence flowcell at the

575 Northwest Genomics Sequencing Core at the University of Washington, Seattle.

576 Data were processed using the Quantitative Insights Into Microbial Ecology 2 (QIIME2)

577 platform [132] using the demux command to demultiplex raw reads and the DADA2 pipeline [133]

578 to generate amplicon sequence variants (ASVs) feature tables. Forward and reverse reads were

579 trimmed to 220 and 180 bases, respectively, to remove the low-quality portion of the sequences.

580 Only samples with more than 20,000 reads were retained for analyses following observation of

581 rarefaction curves. After filtering, trimming, merging, and chimera removal, we retained a total of

582 219,125,888 reads across the 525 immature fecal samples (417,382±645,328 reads per sample,

583 range= 21,256- 7,976,983) and 293,003,271 reads across the 620 adult female fecal samples

584 (472,586±869,181reads per sample, range= 20,068- 10,723,460). ASVs were taxonomically

585 assigned using the q2-feature classifier in QIIME2 against version 132 of the SILVA database

586 (updated December 2017) [134] based on 100% similarity.

587

588 ***Statistical analyses***

589 The count and taxonomy files generated by QIIME2 were imported into R version 3.5.2 [135]

590 using the qiime2R package [136]. We filtered the count table to retain only ASVs that had at least

591 500 reads total in the dataset to eliminate potentially artifactual sequences. With this filtering

592 criteria, only 3,884 ASVs remained (out of the 29,686 initially observed). In total, 3,784 different

593 ASVs were found across the 525 immature fecal samples (mean±SD number of ASVs per sample:

594 728±261, range: 65-1498), while the 620 female samples contained 3,679 ASVs (mean±SD

595 number of ASVs per sample: 829±248, range: 98-1761). Most ASVs could be taxonomically

596 assigned to the phylum (100%), class (99%), and order levels (99%), with assignments decreasing

597 substantially at the family (88%) and genus (63%) levels.

598

599 <u>Alpha-diversity analyses</u>

600 We calculated three complementary metrics of alpha diversity for each sample: the observed

601 richness (the total number of unique ASVs per sample), Shannon Index (taking into account both

602 richness and evenness in abundance of ASVs), and Faith's phylogenetic diversity (a measure of

603 the diversity of phylogenetic lineages within a sample) using the "phyloseq" [137] and "picante"

604 package [138]. To assess which predictors affected immatures' gut microbial alpha diversity, we

605 used generalized additive mixed models (GAMMs) with the 'mgcv' package in R [139]. Such

606 models allow fitting of a nonlinear relationship between the response variable and the fixed effect

607 (by adding a smooth term), such as between alpha diversity and immature age (**Figure 1C**). Fitted

608 predictors included: immature age at the date of fecal sample collection (modeled as a smooth

609 term), immature sex, the parity status of mother, maternal dominance rank in the month of infant's

610 birth, cumulative monthly rainfall, average monthly minimum temperature and the log-

611 transformed sequencing depth (i.e., the number of reads per sample). The use of rarefaction (i.e.,

612 subsampling of the read counts in each sample to a common sequencing depth) has been strongly

613 discouraged on microbiome dataset because it discards too much sequencing information and leads

614 to high rate of false positives [140], so we calculated alpha diversity on raw counts but controlled

615 for sequencing depth in our model. Graphical representation of alpha diversity metrics are

616 nonetheless displayed using a rarefied dataset at 20,000 reads. Individual identity and unit

617 membership were included as random effects. Model residual checks were performed using the

618 qq.gamViz and check.gamViz functions. Given that GAMMs models can not accommodate the

619   test of the interaction between a smooth and fixed term, we ran those models including all

620   immature samples or on only young infants (0-12 months) to test for the significance of maternal

621   effects in early life (i.e., when the infant is still nursing).

622   To quantitatively assess the age at which alpha diversity reaches a plateau (i.e., converges

623   to adult-like pattern), we used quadratic plateau models (formula: $y \sim (a + b * x + c * I(x^2)) * (x$

624   $\leq -0.5 * b/c) + (a + I(-b^2/(4 * c))) * (x > -0.5 * b/c))$ fitted using the nlsfit() function of the

625   easynls package [141] and extracted the critical point of inflexion and r-squared of the optimized

626   model (i.e., with the values of a, b and c fit best the data). Since it is not possible to control for

627   covariates in those analyses (e.g., sequencing depth), we ran those models on a rarefied dataset at

628   20,000 reads.

629

630   <u>Beta-diversity analyses</u>

631   Beta-diversity (between-sample dissimilarity in composition) was computed as the Aitchison

632   distance [142], which is simply the Euclidean distance between samples after centered log-ratio

633   (clr) transformation of the raw counts (a pseudo-count was added to the zeros using the imputation

634   based on a Bayesian-multiplicative replacement from the cmultRepl() function in the package

635   zCompositions [143]). The clr transformation allows us to account for differences in sequencing

636   depth between samples and is a better practice than rarefaction of the counts [144]. Principal

637   components analysis (PCA) on the Aitchison dissimilarity matrix (function "prcomp") was used

638   to examine how immatures samples clustered by age. We extracted the loading scores for each

639   ASV onto the first Principal component (PC1) of the PCA to determine which specific ASVs have

640   the highest influence on the clustering by age of samples. A quadratic plateau model was

641   implemented to find the age at which Aitchison beta diversity reaches a plateau.

642   Permutational Multivariate Analysis of Variance (PERMANOVA) was then carried out on

643   the Aitchison dissimilarity matrix using the adonis2 function in the vegan package [145] (with

644   10,000 permutations) to test for associations among gut microbial beta-diversity and the variables

645   of interest (immature age, sex, maternal parity, maternal rank, environmental variables, the log-

646   transformed sequencing depth, and unit membership). Individual identity was included as a

647   blocking factor ("strata") to control for repeated sampling among individuals. PERMANOVA

648   models were run when including all immatures samples or on only young infants (0-12 months) to

649   test for the significance of maternal effects in early life. We also replicated those PERMANOVA

650   analyses using more classical measures of beta diversity (unweighted and weighted UniFrac

651   dissimilarity) on a rarefied dataset at 20,000 reads and found essentially similar results (**Table**

652   **S13**).

653

654   Mother-infant comparison of gut microbiome composition

655   To assess similarity in gut microbiome composition between mother and offspring, we calculated

656   (1) the number of shared ASVs across maternal and immature communities, and (2) the beta

657   diversity dissimilarity (unweighted and weighted UniFrac distances) between the matched infant-

658   mother fecal samples collected the same day (N=398). The dataset of immature and mother fecal

659   samples was rarefied at 20,000 reads to calculate these metrics since sequencing depth is likely to

660   affect the similarity between paired samples. Quadratic plateau models were implemented on the

661   three metrics to identify the age at which infants converged toward the maternal (i.e., adult-like)

662   gut microbial composition. To assess which predictors affected the compositional similarity

663   between mother-offspring pairs, we used GAMMs to model those three metrics as a function of

664   immature age (as a smooth term), immature sex, maternal parity and maternal dominance rank,

665   climatic variables (cumulative monthly rainfall and average monthly minimum temperature),

666   while individual identity and unit membership were included as random effects. These GAMMs

667   were also run separately on young infant samples (<12 months) or only on old immatures (>18

668   months) to assess how the strength of vertical transmission varies with maternal traits.

669

670   <u>Individuality of the microbiomes in immatures</u>

671   To capture the compositional divergence between immature samples, we calculated a measure of

672   "individuality" of the microbiomes among the 525 immature samples, as defined in [146], which

673   corresponds to the beta diversity dissimilarity value between a sample and the most similar sample

674   (i.e., the minimum pairwise values from a beta diversity dissimilarity matrix, based on unweighted

675   and weighted UniFrac metrics). The higher the value, the more distinct the gut microbiome

676   composition is from all other immature samples in the cohort. This was calculated using the

677   rarefied dataset at 20,000 reads.

678

679   <u>Age-associated changes in microbial taxonomic composition</u>

680   To identify the microbial taxa that vary significantly in abundance as immatures age, we used a

681   statistical framework that is commonly used to analyze time series (and, in our case, longitudinal

682   dataset). Autoregressive Integrated Moving Average (ARIMA) models allowed us to model and

683   test for chronological trends in temporal data [147]. First, raw microbial counts were aggregated

684   at the family or genus level, normalized using a clr-transformation, and z-transformed per taxon

685   (i.e., across samples) to correct for variation in library size and unaccounted variance due to other

686   covariates. Only microbial families or genera $\geq 0.01\%$ relative abundance across the samples were

687   selected for further analyses. Second, the counts were averaged across samples belonging to the

688   same chronological age and converted into z-ordered objects (using R package zoo [148]) and into

689   time series objects. Formatted time series were then analyzed using auto.arima (from the forecast

690   R package [149]), using stepwise search and Akaike Information Criterion (AIC) to select the best

691   model. This algorithm scans a wide range of possible ARIMA models and selects the one with the

692   smallest AIC. ARIMA models that exhibited significant non-stationary trends (as opposed to

693   unstructured "noise" fluctuations indistinguishable from stationary data) were selected following

694   the criteria in [147]: (1) the difference order from stationary was higher than zero, and (2) at least

695   one autoregressive (AR) and moving average (MA) coefficient was included in the model. LOESS

696   regressions were then fitted to re-predict the count of each taxon as a function of age.

697   We then grouped bacterial taxa into clusters based on similarities in age-associated

698   abundance trajectories. Pairwise distances between microbial taxa trajectories (i.e., the predicted

699   values of the LOESS regression) were computed using correlation coefficients as a distance

700   measure [150], and hierarchical clustering was performed using the complete method (using the

701   function hclust from the stats R package). The optimal number of clusters was determined using

702   the Elbow method (i.e., choosing a number of clusters so that adding another cluster does not

703   highly improve the total within-cluster sum of squares) [151]. Results of hierarchical clustering

704   were visualized using the R package heatmap3 [152] to provide an overview of gut microbiome

705   composition changes with age.

706

707   <u>Age-associated changes in microbial functional composition</u>

708   To predict the microbial functional metagenomes of each sample from 16S rRNA data, we used

709   Phylogenetic Investigation of Communities by Reconstruction of Unobserved States 2

710   (PICRUSt2) v.2.1.3-b software [84] with default options (picrust2_pipeline.py). We then

711   computed the relative abundance of Kyoto Encyclopedia of Genes and Genomes (KEGG)

712   Orthologs (KOs) (agglomerated at level 2 or 3 of the BRITE map) and of Enzyme Commission

713   (EC) numbers for each sample. The accuracy of the PICRUSt2 predictions for each sample were

714   assessed by calculating the weighted Nearest Sequence Taxon Index (NSTI) score, a measure of

715   how similar the bacteria from the sample are to reference genome sequences. The mean±SD NSTI

716   score across the 525 immature samples was 0.49 ± 0.19 (range: 0.01-0.89).

717   The age-related temporal trajectory of each KO pathway and EC was assessed using

718   ARIMA models in a similar fashion than described above. The only difference is that the raw

719   metagenome counts were transformed into relative abundance (instead of clr transformed). Only

720   microbial pathways $\geq 0.01\%$ relative abundance across the samples were included. Hierarchical

721   clustering was used to group the pathways with similar aging trajectories.

722

723   <u>Maternal effects on offspring's gut microbiome development</u>

724   We examined how maternal traits (dominance rank, parity) were associated with differences in

725   offspring gut microbiome (1) composition (at the family and genus levels) and (2) function (KO

726   pathways at level 2 or 3 and EC numbers) using GAMMs models. We modelled the relative

727   abundance of each taxon and each functional pathway as a function of maternal parity and maternal

728   dominance rank in the month of infant's birth, while controlling for immature age (as a smooth

729   term), immature sex, climatic variables (cumulative monthly rainfall and average monthly

730   minimum temperature. For (1), the logarithm of the relative abundance of each taxon was fit

731   (adding a pseudo-count of 0.001% to include zero counts). In all models, individual identity and

732   unit membership were included as random effects. P-values were adjusted for multiple hypothesis

733   testing by calculating the Benjamini-Hochberg FDR multiple-test correction. Only taxa that had

734   an average relative abundance across samples $\geq 0.01\%$ were tested. Given the number of metabolic

735   pathways and the correction of p-values for multiple testings, only pathways that had an average

736   relative abundance across samples $\geq 0.10\%$ were tested. Taxa or functional pathways with a p-

737   value < 0.05 were considered statistically significant. These analyses were run including all

738   immatures samples (0-3 years), only young infant samples (<12months) or only old samples (>18

739   months).

740

741   <u>Mother-to-infant vertical transmission</u>

742   To assess if maternal and infant gut microbiome communities were more similar than expected by

743   chance, we took a resampling approach (with 1000 repetitions) to compare the number of shared

744   ASVs and beta diversity dissimilarity metrics (unweighted and weighted UniFrac) between (1)

745   actual mother-infant matched samples (the observed value) and (2) random pairs of fecal samples

746   of an infant and an adult female of the population (the random distribution). Since mother-infant

747   pairs always shared the same social unit and were always collected 0-1 day apart (i.e., in the same

748   season), we needed to match the random female samples accordingly to avoid introducing

749   consistent bias in the random distribution. The random matching was thus done by either matching

750   the infant sample to (i) a female of the same unit (to control for higher similarity only due to

751   sharing the same social group) or (ii) a female sample collected in the same season (to control for

752   higher similarity only due to seasonality). We did not have enough female samples to match by

753   both criteria simultaneously. After we created the set of random pairs, we use GAMMs to compare

754   the observed and random distribution of the metrics (number of shared ASVs or beta diversity

755   dissimilarity) (response variable) by fitting a variable ("type of pairs?") coding whether the value

756   comes from an actual mother-offspring pair (1=observed) or a random infant-female pair

757   (0=random), and controlling for immature age (as a smooth term) and immature sex. Infant and

758   female identity were included as random effects to account for repeated observations of the same

759   individuals. We extracted the estimate of the "type of pairs?" variable for the model and re-ran the

760   model on a different set of random pairs (1000 times in total). We thus obtained a distribution of

761   1000 estimates for the "type of pairs?" variable. We report the exact p-value (calculated as the

762   proportion of models with positive estimates for the number of shared ASVs and the proportion of

763   models with negative estimates for beta dissimilarity) and the 95% confidence interval of the

764   estimates of the "type of pairs?" variable. Fecal samples were rarefied at 20,000 reads to control

765   for differences in sequence depth between infant and female samples. These analyses were run

766   including all immatures samples (0-3 years), only young infant samples (0-12 months), or only old

767   immatures (>18 months) to compare the strength of the effect among the different age categories.

768   To examine the nature of the shared microbes between mother and offspring in early life

769   (when infants are <12 months), we extracted all ASVs in common between the 136 mother-

770   offspring pairs (on the rarefied dataset). For each ASV found in the young infant samples (<12

771   months, N=3,402 ASVs total), we simply computed its relative abundance and prevalence across

772   samples and how many pairs shared this given ASV. We then plotted the loading score of the ASV

773   on PC1 of the beta diversity ordination (PC1 correlates strongly with age, so ASVs with the most

774   negative versus positive loading scores are found in early versus later life) according to the

775   percentage of mother-offspring pairs sharing this ASV.

776

ACKNOWLEDGEMENTS

780 support to our long-term research project. We are also very grateful to the Simien Mountains

781 Gelada Research Project field team for their help with field data collection, particularly our

782 primary data collectors (Esheti Jejaw, Ambaye Fanta, Setey Girmay, Atirsaw Adugna, Dereje

783 Bewket) and research assistants in the field (in particular Liz Babbitt, Maddie Melton). We would

784 like to thank Marina Watowich and Dr. Kenneth Chiou for helpful discussions on ARIMA

785 analyses.

786

787 **AUTHORS' CONTRIBUTIONS**

788 Conceptualization, Data curation, Formal analysis, Investigation, Visualization: A.B, A.L., N.S.M;

789 Methodology/Laboratory work: A.B., S.S., A.M., Writing – Original Draft: A.B, A.L., N.S.M;

790 Writing – Review & Editing: all authors; Funding Acquisition: A.L., N.S.M., J.C.B., T.J.B., L.R.;

791 Supervision: A.L. and N.S.M.

792

793 **FUNDING**

794 This research was funded by the National Science Foundation (BCS-1723228, BCS-1723237).

795 The long-term gelada research was supported by the National Science Foundation (BCS-2010309,

796 BCS-0715179, IOS-1255974, IOS-1854359), the National Geographic Society (8100-06, 8989-

797 11, NGS-50409R-18), the Leakey Foundation (A.L., J.B., T.B.), the University of Michigan, Stony

798 Brook University, and Arizona State University.

799

800 **AVAILABILITY OF DATA AND MATERIALS**

801 All 16S sequence data used in this study are available at the NCBI Sequence Read Archive under

802 BioProject ID: PRJNA772269 (http://www.ncbi.nlm.nih.gov/bioproject/772269) for the immature

803   samples **[temporary note: the sequences coming from these samples have been deposited on**

804   **NCBI, but will only be released upon acceptance of the manuscript]** and PRJNA639843

805   (https://www.ncbi.nlm.nih.gov/bioproject/PRJNA639843) for the adult female samples. Data

806   (including the ASV table and metadata) and R code to reproduce all the analyses are available at:

807   https://github.com/GeladaResearchProject/Baniel-et-al_2022_Infant-gut-microbiome.

808

809   **COMPETING INTERESTS**

810   The authors declare no competing interests.

811

812   **REFERENCES**

813   1.   Kurokawa K, Itoh T, Kuwahara T, Oshima K, Toh H, Toyoda A, et al. Comparative
814   metagenomics revealed commonly enriched gene sets in human gut microbiomes. DNA
815   Research. 2007;14: 169–181.

816   2.   Koenig JE, Spor A, Scalfone N, Fricker AD, Stombaugh J, Knight R, et al. Succession of
817   microbial consortia in the developing infant gut microbiome. PNAS. 2011;108: 4578–4585.

818   3.   Palmer C, Bik EM, DiGiulio DB, Relman DA, Brown PO. Development of the human
819   infant intestinal microbiota. PLoS Biol. 2007;5: e177.

820   4.   Guittar J, Shade A, Litchman E. Trait-based community assembly and succession of the
821   infant gut microbiome. Nat Commun. 2019;10: 1–11.

822   5.   Bäckhed F, Roswall J, Peng Y, Feng Q, Jia H, Kovatcheva-Datchary P, et al. Dynamics and
823   stabilization of the human gut microbiome during the first year of life. Cell Host Microbe.
824   2015;17: 690–703.

825   6.   Roswall J, Olsson LM, Kovatcheva-Datchary P, Nilsson S, Tremaroli V, Simon M-C, et al.
826   Developmental trajectory of the healthy human gut microbiota during the first 5 years of
827   life. Cell Host Microbe. 2021;29: 765–776.e3.

828   7.   Sharon I, Morowitz MJ, Thomas BC, Costello EK, Relman DA, Banfield JF. Time series
829   community genomics analysis reveals rapid shifts in bacterial species, strains, and phage
830   during infant gut colonization. Genome Res. 2013. pp. 111–120.

831   8.   de Muinck EJ, Trosvik P. Individuality and convergence of the infant gut microbiota during
832   the first year of life. Nat Commun. 2018;9: 1–8.

9. Mach N, Berri M, Estellé J, Levenez F, Lemonnier G, Denis C, et al. Early-life establishment of the swine gut microbiome and impact on host phenotypes. Environmental microbiology reports. 2015;7: 554–569.

10. Petrullo L, Baniel A, Jorgensen MJ, Sams S, Snyder-Mackler N, Lu A. Early life gut microbiome dynamics mediate maternal effects on infant growth in vervet monkeys. https://www.biorxiv.org/content/10.1101/2021.05.11.443657v1

11. Videvall E, Song SJ, Bensch HM, Strandh M, Engelbrecht A, Serfontein N, et al. Major shifts in gut microbiota during development and its relationship to growth in ostriches. Molecular Ecology. 2019;28: 2653–2667.

12. Sommer F, Bäckhed F. The gut microbiota – masters of host development and physiology. Nat Rev Microbiol. 2013;11: 227–238.

13. Heiss CN, Olofsson LE. The role of the gut microbiota in development, function and disorders of the central nervous system and the enteric nervous system. Journal of neuroendocrinology. 2019;31: e12684.

14. Clarke G, O'Mahony SM, Dinan TG, Cryan JF. Priming for health: gut microbiota acquired in early life regulates physiology, brain and behaviour. Acta Paediatrica. 2014;103: 812–819.

15. Gensollen T, Iyer SS, Kasper DL, Blumberg RS. How colonization by microbiota in early life shapes the immune system. Science. 2016;352: 539–544.

16. Gollwitzer ES, Marsland BJ. Impact of early-life exposures on immune maturation and susceptibility to disease. Trends Immunol. 2015;36: 684–696.

17. Warne RW, Kirschman L, Zeglin L. Manipulation of gut microbiota during critical developmental windows affects host physiological performance and disease susceptibility across ontogeny. Journal of Animal Ecology. 2019;88: 845–856.

18. Arrieta M-C, Stiemsma LT, Amenyogbe N, Brown EM, Finlay B. The intestinal microbiome in early life: health and disease. Front Immunol. 2014;5: 427.

19. Stiemsma LT, Michels KB. The role of the microbiome in the developmental origins of health and disease. Pediatrics. 2018;141.

20. Risnes KR, Belanger K, Murk W, Bracken MB. Antibiotic exposure by 6 months and asthma and allergy at 6 years: findings in a cohort of 1,401 US children. American journal of epidemiology. 2011;173: 310–318.

21. Yallapragada SG, Nash CB, Robinson DT. Early-life exposure to antibiotics, alterations in the intestinal microbiome, and risk of metabolic disease in children and adults. Pediatric Annals. 2015.

22. Rautava S. Early-life antibiotic exposure, the gut microbiome, and disease in later life. The

868   Human microbiome in early Life. Academic Press. 2021. pp. 135–153.

869   23. Ungaro R, Bernstein CN, Gearry R, Hviid A, Kolho K-L, Kronman MP, et al. Antibiotics
870   associated with increased risk of new-onset Crohn's disease but not ulcerative colitis: a
871   meta-analysis. American Journal of Gastroenterology. 2014. pp. 1728–1738.

872   24. Bauer H, Horowitz RE, Levenson SM, Popper H. The response of the lymphatic tissue to
873   the microbial flora. Studies on germfree mice. Am J Pathol. 1963;42: 471–483.

874   25. Olszak T, An D, Zeissig S, Vera MP, Richter J, Franke A, et al. Microbial exposure during
875   early life has persistent effects on natural killer T cell function. Science. 2012;336: 489–
876   493.

877   26. Cox LM, Yamanishi S, Sohn J, Alekseyenko AV, Leung JM, Cho I, et al. Altering the
878   intestinal microbiota during a critical developmental window has lasting metabolic
879   consequences. Cell. 2014;158: 705–721.

880   27. Aidy SE, El Aidy S, Hooiveld G, Tremaroli V, Bäckhed F, Kleerebezem M. The gut
881   microbiota and mucosal homeostasis. Gut Microbes. 2013. pp. 118–124.

882   28. Kozakova H, Schwarzer M, Tuckova L, Srutkova D, Czarnowska E, Rosiak I, et al.
883   Colonization of germ-free mice with a mixture of three *Lactobacillus* strains enhances the
884   integrity of gut mucosa and ameliorates allergic sensitization. Cell Mol Immunol. 2016;13:
885   251–262.

886   29. Moore RE, Townsend SD. Temporal development of the infant gut microbiome. Open Biol.
887   2019;9: 190128.

888   30. Vandenplas Y, Carnielli VP, Ksiazyk J, Luna MS, Migacheva N, Mosselmans JM, et al.
889   Factors affecting early-life intestinal microbiota development. Nutrition. 2020;78: 110812.

890   31. Dwivedi M, Ansarullah, Radichev I, Kemp EH. Alteration of immune-mechanisms by
891   human microbiota and development and prevention of human diseases. J Immunol Res.
892   2017;2017: Article ID 6985256.

893   32. Schloss PD, Schubert AM, Zackular JP, Iverson KD, Young VB, Petrosino JF. Stabilization
894   of the murine gut microbiome following weaning. Gut Microbes. 2012;3: 383–393.

895   33. Charbonneau MR, O'Donnell D, Blanton LV, Totten SM, Davis JCC, Barratt MJ, et al.
896   Sialylated milk oligosaccharides promote microbiota-dependent growth in models of infant
897   undernutrition. Cell. 2016;164: 859–871.

898   34. Foong JPP, Hung LY, Poon S, Savidge TC, Bornstein JC. Early life interaction between the
899   microbiota and the enteric nervous system. Am J Physiol Gastrointest Liver Physiol.
900   2020;319: G541–G548.

901   35. Kennedy EA, King KY, Baldridge MT. Mouse microbiota models: comparing germ-free
902   mice and antibiotics treatment as tools for modifying gut bacteria. Front Physiol. 2018;9:

903   1534.

904   36.   Beaumont M, Paës C, Mussard E, Knudsen C, Cauquil L, Aymard P, et al. Gut microbiota
905   derived metabolites contribute to intestinal barrier maturation at the suckling-to-weaning
906   transition. Gut Microbes. 2020;3: 1–9.

907   37.   Frese SA, Parker K, Calvert CC, Mills DA. Diet shapes the gut microbiome of pigs during
908   nursing and weaning. Microbiome. 2015;3: 28.

909   38.   Meale SJ, Li S, Azevedo P, Derakhshani H, Plaizier JC, Khafipour E, et al. Development of
910   ruminal and fecal microbiomes are affected by weaning but not weaning strategy in dairy
911   calves. Front Microbiol. 2016;7: 582.

912   39.   Berry ASF, Pierdon MK, Misic AM, Sullivan MC, O'Brien K, Chen Y, et al. Remodeling
913   of the maternal gut microbiome during pregnancy is shaped by parity. Microbiome. 2021;9:
914   1–5.

915   40.   Pascoe EL, Hauffe HC, Marchesi JR, Perkins SE. Network analysis of gut microbiota
916   literature: an overview of the research landscape in non-human animal studies. ISME J.
917   2017;11: 2644–2651.

918   41.   Amato KR. Co-evolution in context: The importance of studying gut microbiomes in wild
919   animals. Microbiome Sci Med. 2013;1.

920   42.   Wang S, Ryan CA, Boyaval P, Dempsey EM, Ross RP, Stanton C. Maternal vertical
921   transmission affecting early-life microbiota development. Trends Microbiol. 2020;28: 28–
922   45.

923   43.   McDonald B, McCoy KD. Maternal microbiota in pregnancy and early life. Science.
924   2019;365: 984–985.

925   44.   Ferretti P, Pasolli E, Tett A, Asnicar F, Gorfer V, Fedi S, et al. Mother-to-infant microbial
926   transmission from different body sites shapes the developing infant gut microbiome. Cell
927   Host Microbe. 2018;24: 133–145.e5.

928   45.   Mueller NT, Bakacs E, Combellick J, Grigoryan Z, Dominguez-Bello MG. The infant
929   microbiome development: Mom matters. Trends Mol Med. 2015;21: 109–117.

930   46.   Funkhouser LJ, Bordenstein SR. Mom knows best: the universality of maternal microbial
931   transmission. PLoS Biol. 2013;11: e1001631.

932   47.   Mallott EK, Amato KR. Host specificity of the gut microbiome. Nat Rev Microbiol.
933   2021;19: 639–653.

934   48.   Bokulich NA, Chung J, Battaglia T, Henderson N, Jay M, Li H, et al. Antibiotics, birth
935   mode, and diet shape microbiome maturation during early life. Science Translational
936   Medicine. 2016. pp. 343ra82–343ra82.

49. Jost T, Lacroix C, Braegger CP, Rochat F, Chassard C. Vertical mother-neonate transfer of maternal gut bacteria via breastfeeding. Environ Microbiol. 2014;16: 2891–2904.

50. Pannaraj PS, Li F, Cerini C, Bender JM, Yang S, Rollie A, et al. Association between breast milk bacterial communities and establishment and development of the infant gut microbiome. JAMA Pediatr. 2017;171: 647–654.

51. Zivkovic AM, German JB, Lebrilla CB, Mills DA. Human milk glycobiome and its impact on the infant gastrointestinal microbiota. PNAS. 2011;108: 4653–4658.

52. Pacheco AR, Barile D, Underwood MA, Mills DA. The impact of the milk glycobiome on the neonate gut microbiota. Annu Rev Anim Biosci. 2015;3: 419–445.

53. Newburg DS, Morelli L. Human milk and infant intestinal mucosal glycans guide succession of the neonatal intestinal microbiota. Pediatr Res. 2015;77: 115–120.

54. Murphy K, Curley D, O'Callaghan TF, O'Shea C-A, Dempsey EM, O'Toole PW, et al. The composition of human milk and infant faecal microbiota over the first three months of life: a pilot study. Sci Rep. 2017;7: 40597.

55. Asnicar F, Manara S, Zolfo M, Truong DT, Scholz M, Armanini F, et al. Studying vertical microbiome transmission from mothers to infants by strain-level metagenomic profiling. mSystems. 2017;2.

56. Korpela K, Costea P, Coelho LP, Kandels-Lewis S, Willemsen G, Boomsma DI, et al. Selective maternal seeding and environment shape the human gut microbiome. Genome Res. 2018;28: 561–568.

57. Perez PF, Doré J, Leclerc M, Levenez F, Benyacoub J, Serrant P, et al. Bacterial imprinting of the neonatal immune system: lessons from maternal cells? Pediatrics. 2007;119: e724–32.

58. Sarkar A, Harty S, Johnson KV, Moeller AH, Archie EA, Schell LD, et al. Microbial transmission in animal social networks and the social microbiome. Nature Ecology Evolution. 2020;22: 1–6.

59. Sprockett D, Fukami T, Relman DA. Role of priority effects in the early-life assembly of the gut microbiota. Nat Rev Gastroenterol Hepatol. 2018;15: 197–205.

60. Bogado Pascottini O, Spricigo JFW, Van Schyndel SJ, Mion B, Rousseau J, Weese JS, et al. Effects of parity, blood progesterone, and non-steroidal anti-inflammatory treatment on the dynamics of the uterine microbiota of healthy postpartum dairy cows. PLoS One. 2021;16: e0233943.

61. Marcobal A, Barboza M, Sonnenburg ED, Pudlo N, Martens EC, Desai P, et al. *Bacteroides* in the infant gut consume milk oligosaccharides via mucus-utilization pathways. Cell Host Microbe. 2011;10: 507–514.

62. Marcobal A, Barboza M, Froehlich JW, Block DE, German JB, Lebrilla CB, et al. Consumption of human milk oligosaccharides by gut-related microbes. J Agric Food Chem. 2010;58: 5334–5340.

63. Hinde K, Power ML, Oftedal OT. Rhesus macaque milk: magnitude, sources, and consequences of individual variation over lactation. Am J Phys Anthropol. 2009;138: 148–157.

64. Hinde K, Milligan LA. Primate milk: proximate mechanisms and ultimate perspectives. Evol Anthropol. 2011;20: 9–23.

65. Lu A, Petrullo L, Carrera S, Feder J, Schneider-Crease I, Snyder-Mackler N. Developmental responses to early-life adversity: evolutionary and mechanistic perspectives. Evol Anthropol. 2019;28: 249–266.

66. Stanton MA, Lonsdorf EV, Murray CM, Pusey AE. Consequences of maternal loss before and after weaning in male and female wild chimpanzees. Behav Ecol Sociobiol. 2020;74: 22.

67. Tung J, Archie EA, Altmann J, Alberts SC. Cumulative early life adversity predicts longevity in wild baboons. Nat Commun. 2016;7: 1–7.

68. Zipple MN, Archie EA, Tung J, Altmann J, Alberts SC. Intergenerational effects of early adversity on survival in wild baboons. eLife. 2019;24: e47433.

69. Silk JB, Beehner JC, Bergman TJ, Crockford C, Engh AL, Moscovice LR, et al. The benefits of social capital: close social bonds among female baboons enhance offspring survival. Proc. Royal Soc. B: Biological Sciences. 2009;276: 3099–3104.

70. Maestripieri D. Maternal influences on primate social development. Behav Ecol Sociobiol. 2018;72: 1–12.

71. Altmann J, Alberts SC. Growth rates in a wild primate population: ecological influences and maternal effects. Behav Ecol Sociobiol. 2005;57: 490–501.

72. Stoffel MA, Acevedo-Whitehouse K, Morales-Durán N, Grosser S, Chakarov N, Krüger O, et al. Early sexual dimorphism in the developing gut microbiome of northern elephant seals. Mol Ecol. 2020;29: 2109–2122.

73. Janiak MC, Montague MJ, Villamil CI, Stock MK, Trujillo AE, DePasquale AN, et al. Age and sex-associated variation in the multi-site microbiome of an entire social group of free-ranging rhesus macaques. Microbiome. 2021;9: 1–17.

74. Reese AT, Phillips SR, Owens LA, Venable EM, Langergraber KE, Machanda ZP, et al. Age patterning in wild chimpanzee gut microbiota diversity reveals differences from humans in early life. Curr Biol. 2021;31: 613–620.e3.

75. McKenney EA, Rodrigo A, Yoder AD. Patterns of gut bacterial colonization in three

1007   primate species. PLoS One. 2015;10: e0124618.

1008   76. Jarvey JC, Low BS, Pappano DJ, Bergman TJ, Beehner JC. Graminivory and fallback
1009   foods: annual diet profile of geladas (*Theropithecus gelada*) living in the Simien Mountains
1010   National Park, Ethiopia. Int J Primatol. 2018;39: 105–126.

1011   77. Fashing PJ, Nguyen N, Venkataraman VV, Kerby JT. Gelada feeding ecology in an intact
1012   ecosystem at Guassa, Ethiopia: Variability over time and implications for theropith and
1013   hominin dietary evolution. Am J Phys Anthropol. 2014;155: 1–16.

1014   78. Trosvik P, de Muinck EJ, Rueness EK, Fashing PJ, Beierschmitt EC, Callingham KR, et al.
1015   Multilevel social structure and diet shape the gut microbiota of the gelada monkey, the only
1016   grazing primate. Microbiome. 2018;6: 84.

1017   79. Baniel A, Amato KR, Beehner JC, Bergman TJ, Mercer A, Perlman RF, et al. Seasonal
1018   shifts in the gut microbiome indicate plastic responses to diet in wild geladas. Microbiome.
1019   2021;9: 1–20.

1020   80. Snyder-Mackler N, Beehner JC, Bergman TJ. Defining higher levels in the multilevel
1021   societies of geladas (*Theropithecus gelada*). Int J Primatol. 2012;33: 1054–1068.

1022   81. Roberts EK, Lu A, Bergman TJ, Beehner JC. Female reproductive parameters in wild
1023   geladas (*Theropithecus gelada*). Int J Primatol. 2017;38: 1–20.

1024   82. Milani C, Duranti S, Bottacini F, Casey E, Turroni F, Mahony J, et al. The first microbial
1025   colonizers of the human gut: composition, activities, and health implications of the infant
1026   gut microbiota. Microbiol Mol Biol Rev. 2017;81: 1–67.

1027   83. Derrien M, Alvarez A-S, de Vos WM. The gut microbiota in the first decade of life. Trends
1028   Microbiol. 2019;27: 997–1010.

1029   84. Douglas GM, Maffei VJ, Zaneveld JR, Yurgel SN, Brown JR, Taylor CM, et al. PICRUSt2
1030   for prediction of metagenome functions. Nat Biotechnol. 2020;38: 685–688.

1031   85. Korpela K, de Vos WM. Early life colonization of the human gut: microbes matter
1032   everywhere. Curr Opin Microbiol. 2018;44: 70–78.

1033   86. Cavalli C, Teng C, Battaglia FC, Bevilacqua G. Free sugar and sugar alcohol concentrations
1034   in human breast milk. J Pediatr Gastroenterol Nutr. 2006;42: 215–221.

1035   87. Fox JG, Boutin SR, Handt LK, Taylor NS, Xu S, Rickman B, et al. Isolation and
1036   characterization of a novel *Helicobacter* species, "*Helicobacter macacae*", from rhesus
1037   monkeys with and without chronic idiopathic colitis. Journal of Clinical Microbiology.
1038   2007. pp. 4061–4063.

1039   88. Nielsen HL, Engberg J, Ejlertsen T, Nielsen H. Clinical manifestations of *Campylobacter
1040   concisus* infection in children. Pediatr Infect Dis J. 2013;32: 1194–1198.

1041 89. Klein BS, Vergeront JM, Blaser MJ, Edmonds P, Brenner DJ, Janssen D, et al.
1042   *Campylobacter* infection associated with raw milk. An outbreak of gastroenteritis due to
1043   *Campylobacter jejuni* and thermotolerant *Campylobacter fetus* subsp *fetus*. JAMA.
1044   1986;255: 361–364.

1045 90. Aureli P, Fenicia L, Pasolini B, Gianfranceschi M, McCroskey LM, Hatheway CL. Two
1046   cases of type E infant botulism caused by neurotoxigenic *Clostridium butyricum* in Italy. J
1047   Infect Dis. 1986;154: 207–211.

1048 91. Rood JI, Cole ST. Molecular genetics and pathogenesis of *Clostridium perfringens*.
1049   Microbiol Rev. 1991;55: 621–648.

1050 92. Png CW, Lindén SK, Gilshenan KS, Zoetendal EG, McSweeney CS, Sly LI, et al.
1051   Mucolytic bacteria with increased prevalence in IBD mucosa augment in vitro utilization of
1052   mucin by other bacteria. Am J Gastroenterol. 2010;105: 2420–2428.

1053 93. Bergström A, Skov TH, Bahl MI, Roager HM, Christensen LB, Ejlerskov KT, et al.
1054   Establishment of intestinal microbiota during early life: a longitudinal, explorative study of
1055   a large cohort of Danish infants. Appl Environ Microbiol. 2014;80: 2889–2900.

1056 94. Le Doare K, Holder B, Bassett A, Pannaraj PS. Mother's milk: a purposeful contribution to
1057   the development of the infant microbiota and immunity. Front Immunol. 2018;9: 361.

1058 95. Yassour M, Vatanen T, Siljander H, Hämäläinen A-M, Härkönen T, Ryhänen SJ, et al.
1059   Natural history of the infant gut microbiome and impact of antibiotic treatment on bacterial
1060   strain diversity and stability. Sci Transl Med. 2016;8: 343ra81.

1061 96. Pham VT, Lacroix C, Braegger CP, Chassard C. Early colonization of functional groups of
1062   microbes in the infant gut. Environ Microbiol. 2016;18: 2246–2258.

1063 97. Vaishampayan PA, Kuehl JV, Froula JL, Morgan JL, Ochman H, Francino MP.
1064   Comparative metagenomics and population dynamics of the gut microbiota in mother and
1065   infant. Genome Biol Evol. 2010;2: 53–66.

1066 98. Marcobal A, Sonnenburg JL. Human milk oligosaccharide consumption by intestinal
1067   microbiota. Clin Microbiol Infect. 2012;18: 12–15.

1068 99. Yatsunenko T, Rey FE, Manary MJ, Trehan I, Dominguez-Bello MG, Contreras M, et al.
1069   Human gut microbiome viewed across age and geography. Nature. 2012;486: 222–227.

1070 100. Favier CF, Vaughan EE, De Vos WM, Akkermans ADL. Molecular monitoring of
1071   succession of bacterial communities in human neonates. Applied and Environmental
1072   Microbiology. 2002. pp. 219–226.

1073 101. Inoue R, Ushida K. Vertical and horizontal transmission of intestinal commensal bacteria
1074   in the rat model. FEMS Microbiol Ecol. 2003;46: 213–219.

1075 102. Hopkins MJ, Macfarlane GT, Furrie E, Fite A, Macfarlane S. Characterisation of

1076   intestinal bacteria in infant stools using real-time PCR and northern hybridisation analyses.
1077   FEMS Microbiol Ecol. 2005;54: 77–85.

1078   103.   Urashima T, Odaka G, Asakuma S, Uemura Y, Goto K, Senda A, et al. Chemical
1079   characterization of oligosaccharides in chimpanzee, bonobo, gorilla, orangutan, and
1080   siamang milk or colostrum. Glycobiology. 2009;19: 499–508.

1081   104.   Urashima T, Asakuma S, Leo F, Fukuda K, Messer M, Oftedal OT. The predominance of
1082   type I oligosaccharides is a feature specific to human breast milk. Adv Nutr. 2012;3: 473S–
1083   82S.

1084   105.   Tao N, Wu S, Kim J, An HJ, Hinde K, Power ML, et al. Evolutionary glycomics:
1085   characterization of milk oligosaccharides in primates. J Proteome Res. 2011;10: 1548–1557.

1086   106.   Louis P, Flint HJ. Formation of propionate and butyrate by the human colonic
1087   microbiota. Environ Microbiol. 2017;19: 29–41.

1088   107.   Burger-van Paassen N, Vincent A, Puiman PJ, van der Sluis M, Bouma J, Boehm G, et
1089   al. The regulation of intestinal mucin MUC2 expression by short-chain fatty acids:
1090   implications for epithelial protection. Biochem J. 2009;420: 211–219.

1091   108.   Rivera-Chávez F, Zhang LF, Faber F, Lopez CA, Byndloss MX, Olsan EE, et al.
1092   Depletion of butyrate-producing *Clostridia* from the gut microbiota drives an aerobic
1093   luminal expansion of *Salmonella*. Cell Host Microbe. 2016;19: 443–454.

1094   109.   Chang PV, Hao L, Offermanns S, Medzhitov R. The microbial metabolite butyrate
1095   regulates intestinal macrophage function via histone deacetylase inhibition. PNAS.
1096   2014;111: 2247–2252.

1097   110.   Millard AL, Mertes PM, Ittelet D, Villard F, Jeannesson P, Bernard J. Butyrate affects
1098   differentiation, maturation and function of human monocyte-derived dendritic cells and
1099   macrophages. Clin Exp Immunol. 2002;130: 245–255.

1100   111.   Rokhsefat S, Lin A, Comelli EM. Mucin-microbiota interaction during postnatal
1101   maturation of the intestinal ecosystem: clinical implications. Dig Dis Sci. 2016;61: 1473–
1102   1486.

1103   112.   Vatanen T, Kostic AD, d'Hennezel E, Siljander H, Franzosa EA, Yassour M, et al.
1104   Variation in microbiome LPS immunogenicity contributes to autoimmunity in humans.
1105   Cell. 2016;165: 1551.

1106   113.   Laforest-Lapointe I, Arrieta M-C. Patterns of early-life gut microbial colonization during
1107   human immune development: an ecological perspective. Front Immunol. 2017;8: 788.

1108   114.   Mazmanian SK, Liu CH, Tzianabos AO, Kasper DL. An immunomodulatory molecule of
1109   symbiotic bacteria directs maturation of the host immune system. Cell. 2005;122: 107–118.

1110   115.   Round JL, Mazmanian SK. Inducible Foxp3+ regulatory T-cell development by a

1111   commensal bacterium of the intestinal microbiota. PNAS. 2010;107: 12204–12209.

1112   116.   Telesford KM, Yan W, Ochoa-Reparaz J, Pant A, Kircher C, Christy MA, et al. A
1113   commensal symbiotic factor derived from Bacteroides fragilis promotes human
1114   CD39+Foxp3+ T cells and Treg function. Gut Microbes. 2015;6: 234–242.

1115   117.   Troy EB, Kasper DL. Beneficial effects of *Bacteroides fragilis* polysaccharides on the
1116   immune system. Front Biosci. 2010;15: 25–34.

1117   118.   Schwab C, Gänzle M. Lactic acid bacteria fermentation of human milk oligosaccharide
1118   components, human milk oligosaccharides and galactooligosaccharides. FEMS Microbiol
1119   Lett. 2011;315: 141–148.

1120   119.   Ward RE, Niñonuevo M, Mills DA, Lebrilla CB, German JB. In vitro fermentation of
1121   breast milk oligosaccharides by *Bifidobacterium infantis* and *Lactobacillus gasseri*. Appl
1122   Environ Microbiol. 2006;72: 4497–4499.

1123   120.   Tsuboi KK, Kwong LK, Neu J, Sunshine P. A proposed mechanism of normal intestinal
1124   lactase decline in the postweaned mammal. Biochem Biophys Res Commun. 1981;101:
1125   645–652.

1126   121.   Korpela K. Diet, microbiota, and metabolic Health: trade-off between saccharolytic and
1127   proteolytic fermentation. Annu Rev Food Sci Technol. 2018;9: 65–84.

1128   122.   Ren T, Boutin S, Humphries MM, Dantzer B, Gorrell JC, Coltman DW, et al. Seasonal,
1129   spatial, and maternal effects on gut microbiome in wild red squirrels. Microbiome. 2017;5:
1130   163.

1131   123.   Moeller AH, Foerster S, Wilson ML, Pusey AE, Hahn BH, Ochman H. Social behavior
1132   shapes the chimpanzee pan-microbiome. Science Advances. 2016;2: e1500997.

1133   124.   Grieneisen L, Dasari M, Gould TJ, Björk JR, Grenier J-C, Yotova V, et al. Gut
1134   microbiome heritability is nearly universal but environmentally contingent. Science.
1135   2021;373: 181–186.

1136   125.   Tung J, Barreiro LB, Burns MB, Grenier JC, Lynch J, Grieneisen LE, et al. Social
1137   networks predict gut microbiome composition in wild baboons. eLife. 2015; e05224.

1138   126.   Blekhman R, Tang K, Archie EA, Barreiro LB, Johnson ZP, Wilson ME, et al. Common
1139   methods for fecal sample storage in field studies yield consistent signatures of individual
1140   identity in microbiome sequencing data. Sci Rep. 2016;6: 1–5.

1141   127.   Albers PCH, de Vries H. Elo-rating as a tool in the sequential estimation of dominance
1142   strengths. Anim Behav. 2001;61: 489–495.

1143   128.   Neumann C, Duboscq J, Dubuc C, Ginting A, Irwan AM, Agil M, et al. Assessing
1144   dominance hierarchies: validation and advantages of progressive evaluation with Elo-rating.
1145   Anim Behav. 2011;82: 911–921.

129.   Puff C, Nemomissa S. Plants of the Simen: a flora of the Simen Mountains and surroundings, northern Ethiopia. National Botanic Garden (Belgium); 2005.

130.   Tinsley Johnson E, Snyder-Mackler N, Lu A, Bergman TJ, Beehner JC. Social and ecological drivers of reproductive seasonality in geladas. Behav Ecol. 2018;29: 574–588.

131.   Gohl DM, Vangay P, Garbe J, MacLean A, Hauge A, Becker A, et al. Systematic improvement of amplicon marker gene methods for increased accuracy in microbiome studies. Nat Biotechnol. 2016;34: 942–949.

132.   Bolyen E, Rideout JR, Dillon MR, Bokulich NA, Abnet CC, Al-Ghalith GA, et al. Reproducible, interactive, scalable and extensible microbiome data science using QIIME 2. Nat Biotechnol. 2019;37: 852–857.

133.   Callahan BJ, McMurdie PJ, Rosen MJ, Han AW, Johnson AJA, Holmes SP. DADA2: High-resolution sample inference from Illumina amplicon data. Nat Methods. 2016;13: 581–583.

134.   Quast C, Pruesse E, Yilmaz P, Gerken J, Schweer T, Yarza P, et al. The SILVA ribosomal RNA gene database project: improved data processing and web-based tools. Nucleic Acids Res. 2013;41: D590–6.

135.   Team RC. R: A language and environment for statistical computing. Vienna; 2015.

136.   Bisanz JE. qiime2R: Importing QIIME2 artifacts and associated data into R sessions. Version 0 99. 2018;13.

137.   McMurdie PJ, Holmes S. phyloseq: an R package for reproducible interactive analysis and graphics of microbiome census data. PLoS One. 2013;8: e61217.

138.   Kembel SW, Cowan PD, Helmus MR, Cornwell WK, Morlon H, Ackerly DD, et al. Picante: R tools for integrating phylogenies and ecology. Bioinformatics. 2010;26: 1463–1464.

139.   Wood SN. Stable and efficient multiple smoothing parameter estimation for Generalized Additive Models. J Am Stat Assoc. 2004;99: 673–686.

140.   McMurdie PJ, Holmes S. Waste not, want not: why rarefying microbiome data is inadmissible. PLoS Comput Biol. 2014;10: e1003531.

141.   Arnhold E. easynls: Easy nonlinear model. R Package Version 5.0, 1--9. 2017.

142.   Aitchison J. The Statistical Analysis of Compositional Data. J R Stat Soc Series B Stat Methodol. 1982;44: 139–160.

143.   Palarea-Albaladejo J, Martín-Fernández JA. zCompositions – R package for multivariate imputation of left-censored data under a compositional approach. Chemometrics and Intelligent Laboratory Systems. 2015. pp. 85–96.

1180   144.   Gloor GB, Macklaim JM, Pawlowsky-Glahn V, Egozcue JJ. Microbiome datasets are
1181   compositional: and this is not optional. Front Microbiol. 2017;8: 2224.

1182   145.   Oksanen J, Blanchet FG, Kindt R, Legendre P, O'hara RB, Simpson GL, et al. Vegan:
1183   community ecology package. R package version 1.17-4. URL http://CRAN R-project
1184   org/package= vegan. 2010; 1–5.

1185   146.   Wilmanski T, Diener C, Rappaport N, Patwardhan S, Wiedrick J, Lapidus J, et al. Gut
1186   microbiome pattern reflects healthy ageing and predicts survival in humans. Nature
1187   Metabolism. 2021;3: 274–286.

1188   147.   Márquez EJ, Chung C-H, Marches R, Rossi RJ, Nehar-Belaid D, Eroglu A, et al. Sexual-
1189   dimorphism in human immune system aging. Nat Commun. 2020;11: 1–17.

1190   148.   Zeileis A, Grothendieck G. zoo: S3 infrastructure for regular and irregular time series.
1191   Journal of Statistical Software. 2005.

1192   149.   Hyndman RJ, Khandakar Y. Automatic time series forecasting: the forecast package for
1193   R. Journal of Statistical Software. 2008;27: 1–22.

1194   150.   Tiessen A, Cubedo-Ruiz EA, Winkler R. Improved representation of biological
1195   information by using correlation as distance function for heatmap cluster analysis. Am J
1196   Plant Sci. 2017;08: 502–516.

1197   151.   Syakur MA, Khotimah BK, Rochman EMS, Satoto BD. Integration K-means clustering
1198   method and Elbow method for identification of the best customer profile cluster. IOP Conf
1199   Ser: Mater Sci Eng. 2018;336: 012017.

1200   152.   Zhao S, Guo Y, Sheng Q, Shyr Y. Heatmap3: an improved heatmap package with more
1201   powerful and convenient features. BMC Bioinformatics. 2014;15: P16.
1202

Figure Legends

Figure 1. Gut microbiome taxonomic assembly in the first three years of life in immature geladas.

(A, B) Taxonomic composition of the immature gelada gut microbiome at the phylum and family level as a function of age. The relative abundance of each taxon was calculated per sample by dividing the counts of the taxa by sequencing depth, and then averaged across samples belonging to the age category of interest. Age was split into categories for visualization purposes, but analyses treated age as a continuous variable. (C) Age-associated pattern of alpha diversity within samples, as calculated by the Shannon index (richness and evenness of Amplicon Sequencing Variants, ASVs). The vertical line represents the critical point of inflexion (calculated using quadratic plateau models) representing the age at which alpha diversity converges to adult-like patterns. The dataset was rarefied at 20,000 reads for the figure. (D,E) Age-associated pattern of beta diversity. A Principal Component Analysis (PCA) was used to ordinate the samples based on the Aitchison dissimilarity index (which is simply the Euclidean distance after centered-log-ratio transformation of the raw counts). Panel D represents the projection of the first principal component (PC1) that is best explained by the age of immatures. The vertical line represents the critical point of inflexion (calculated using quadratic plateau models) representing the age at which beta diversity converges to adult-like patterns. Panel E shows how age structures the gut microbiome composition of immatures on the two first principal components. (F) Comparison of gut microbiome composition between mother and offspring, as assessed using 398 matched mother-infant pairs of fecal samples collected on the same day. Here, the number of shared ASVs between pairs of samples is represented. The vertical line represents the critical point of inflexion (calculated using quadratic

1226   plateau models) representing the age at which the number of shared ASVs stabilizes to its maximal

1227   value. The dataset was rarefied at 20,000 reads for the calculation. (G) Age distribution inter-

1228   individual variability in gut microbiomes using the ASV-level unweighted and weighted UniFrac

1229   distances. This score was calculated as the minimum pairwise dissimilarity value from a beta

1230   diversity matrix for a given immature sample, and captures how dissimilar a sample is from its

1231   nearest neighbor, given all other gut microbiome samples in the immature cohort. Higher values

1232   indicate a more distinct gut microbiome from the population. The dataset was rarefied at 20,000

1233   reads for the calculation.

1234

1235   **Figure 2. Age-associated changes in microbial composition at the family level.**

1236   (A) Heatmap of the microbial families exhibiting a significant chronological trend as a function of

1237   age (fitted values from ARIMA models and predicted using LOESS regression per taxa as a

1238   function of age). Values represent z-score normalized counts after centered-log-ratio (clr)

1239   transformation. Hierarchical clustering was used to group age-dependent trajectories into four

1240   clusters exhibiting similar chronological trends. Color bars on the left side identify the clusters.

1241   Taxa (i.e. rows) are ordinated on the heatmap using correlation as distance function. All microbial

1242   families above 0.01% abundance were analyzed (N=55) and the 53 that displayed a significant

1243   trend are represented. (B) Relative abundance of 8 functionally important microbial families that

1244   are enriched in early life (belonging to cluster 1), as a function of age. The age-dependent

1245   trajectories were calculated on clr-transformed counts, but here for interpretation purposes we

1246   represent the LOESS regression on the raw relative abundance across samples (same for panels C

1247   and D). (C) Relative abundance of 5 functionally important microbial families that peak in

1248   abundance around 10 months of age (belonging to cluster 2). Relative abundance is represented

1249   on a log-scale to accommodate high and low abundance families together. (D) Relative abundance

1250   of 8 functionally important microbial families that are enriched in later life (belonging to cluster

1251   4). Relative abundance is represented on a log-scale to accommodate high and low abundance

1252   families together.

1253

1254   **Figure 3. Composition of the early-life microbiota at the genus level.**

1255   Relative abundance of functionally important genera in early life, as a function of age. The age-

1256   dependent trajectories were calculated on clr-transformed counts. For visualization purposes

1257   however, we represent the LOESS regression on the raw relative abundance across samples (on a

1258   log-transformed scale).

1259

1260   **Figure 4. Age-associated changes in the functional profile of the gut microbiome of**

1261   **immatures based on predicted KEGG orthologs (KO) metagenomes.**
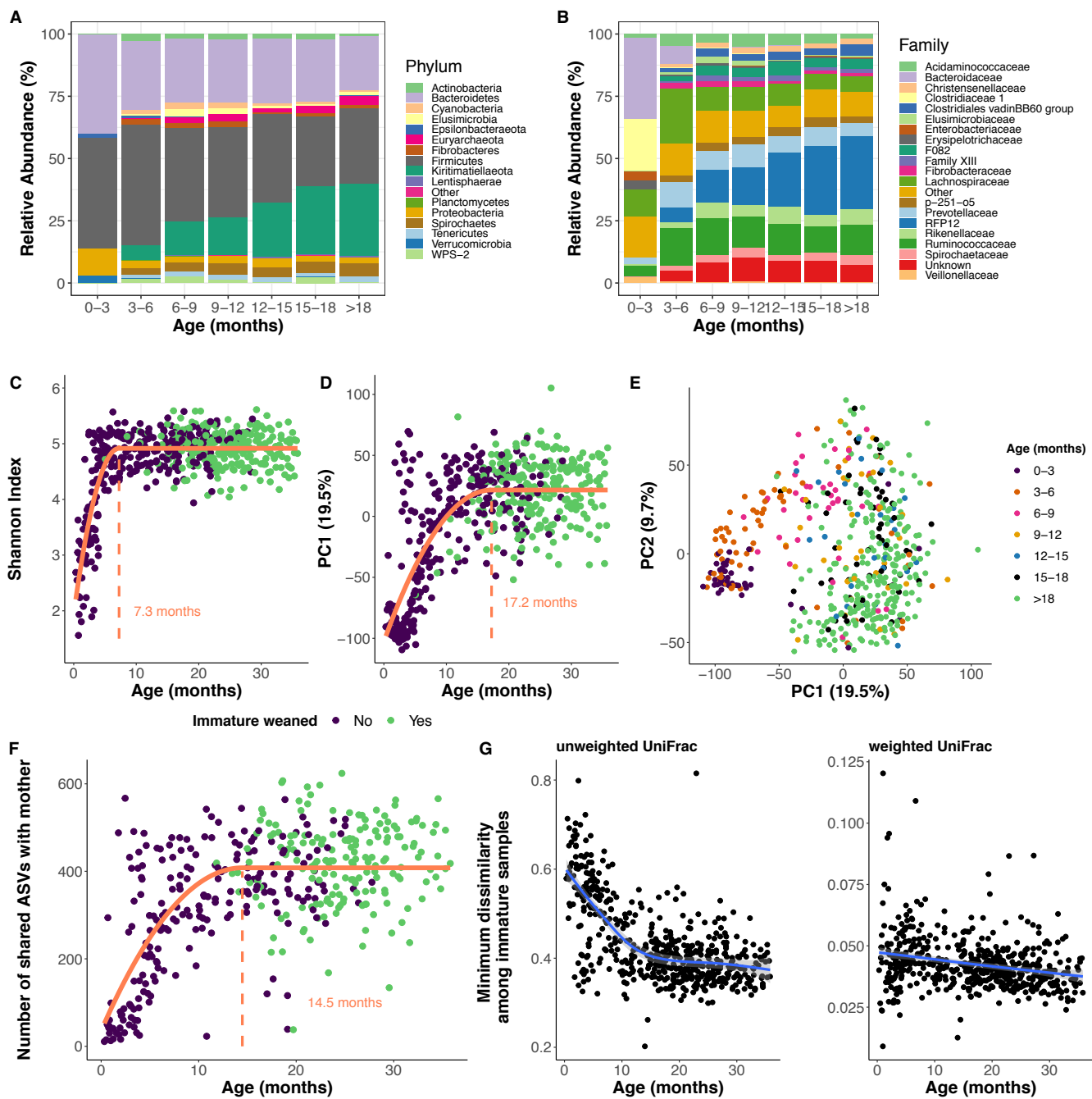
1262   (A) Relative abundance of metabolic pathways (left: KO level 2 and right: KO level 3 of the

1263   carbohydrate metabolism) enriched in early life, as a function of age. (B) Relative abundance of

1264   metabolic pathways (KO level 3) that peak in abundance or decrease in abundance at 10 months

1265   of age. (C) Relative abundance of metabolic pathways (at KO level 2) enriched in later life, as a

1266   function of age. In all plots, the average curve is the LOESS regression on the raw relative

1267   abundance across samples.

1268

1269   **Figure 5. The effect of maternal parity on offspring's gut microbiota functional capacity.**
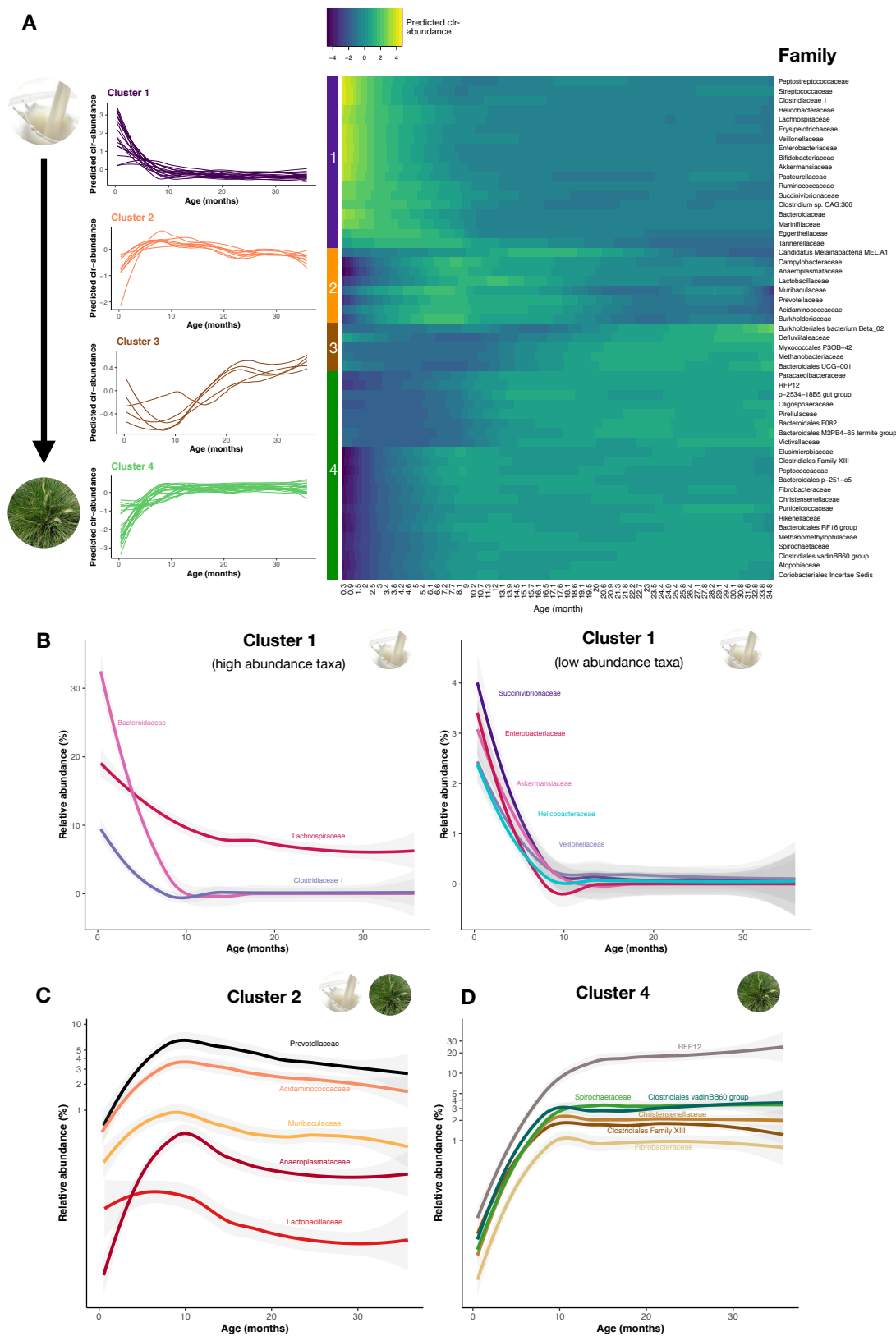
1270   (A) Metabolic pathways (KO level 2 for upper row and KO level 3 for lower row) that are more

1271   abundant in infants <12 months) born to primiparous females than infants of multiparous females.
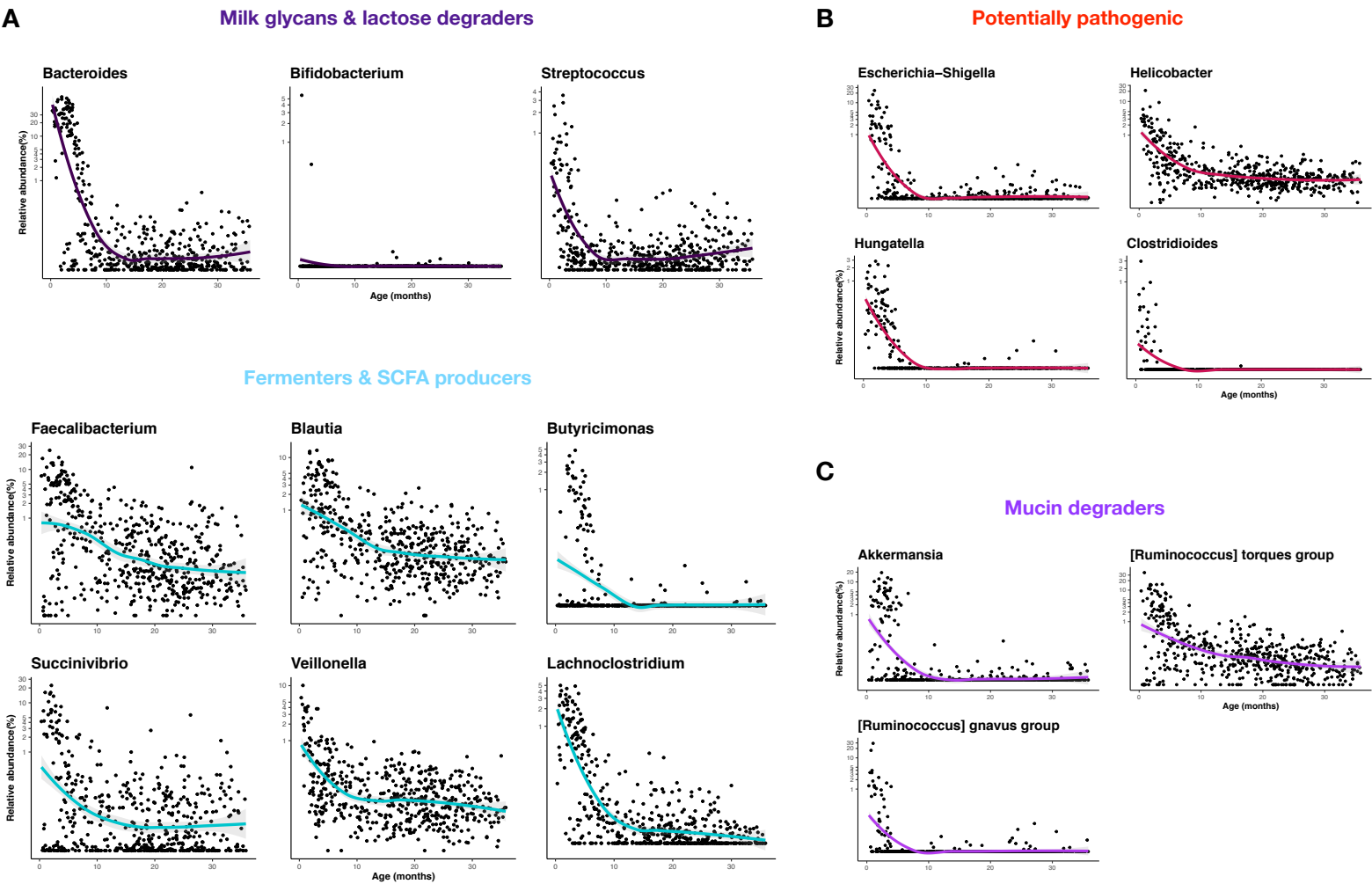
1272   (B) Metabolic pathways (KO level 2) that are less abundant in infants (<12 months) born to

1273   primiparous females than infants of multiparous females. (C) Results of the nonparametric

1274   resampling approach testing if offspring share more Amplicon Sequencing Variants (ASVs) and

1275   have a more similar gut microbiome composition (unweighted UniFrac dissimilarity) to their

1276   mother than to random adult females of the population. The histograms show the random

1277   distribution of the metric of interest (i.e. when matching each infant sample to a random female

1278   sample collected during the same season, with 1000 repetitions). The vertical line shows the

1279   observed value of the metric (i.e. between the actual mother-offspring pairs of fecal samples

1280   collected the same day). This analysis was performed separately on young (nursing) infants (aged

1281   0-12 months, N=136 samples) and old immatures (>18 months, N=201) that were likely weaned.

1282   (D) Composition of the shared ASVs between young infants (<12 months) and their mothers. The

1283   ASVs that are commonly shared between mother-offspring pairs (e.g. among > 70% of the pairs)

1284   in early life tend to have high loading scores of the first principal component (PC1) of a Principal

1285   Component Analysis ordination (based on Aitchison distance). Since PC1 strongly correlates

1286   positively with age, these shared ASVs are characteristic of later life. (E) Vertical transmission

1287   differs for primiparous and multiparous females in early life. Young infants (<12 months) born to

1288   primiparous females share fewer ASVs with their mother and have a more dissimilar gut

1289   microbiome composition (unweighted UniFrac dissimilarity) compared to their mother than

1290   offspring born to multiparous females. Later in life (>18 months), immatures born to primiparous

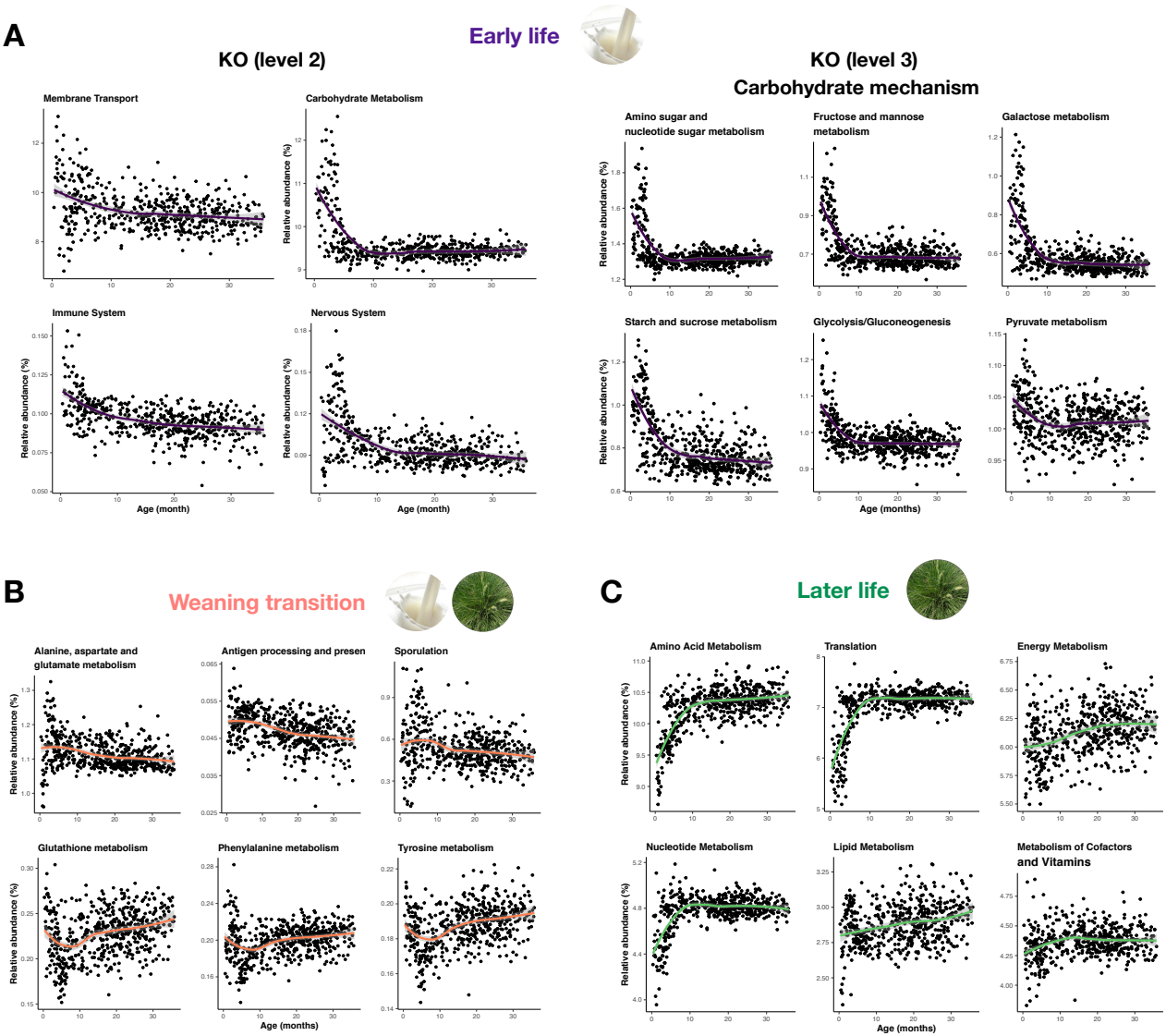1291   and multiparous females are equally similar to their mother in terms of gut microbiome

1292   composition.

1293   **Figure 1.**

1294

1295 **Figure 2.**

1296

1297   **Figure 3.**

A — Milk glycans & lactose degraders

Bacteroides   Bifidobacterium   Streptococcus

Relative abundance(%)

Age (months)

Fermenters & SCFA producers

Faecalibacterium   Blautia   Butyricimonas

Succinivibrio   Veillonella   Lachnoclostridium

Relative abundance(%)

Age (months)

B — Potentially pathogenic

Escherichia–Shigella   Helicobacter

Hungatella   Clostridioides

Relative abundance(%)

Age (months)

C — Mucin degraders

Akkermansia   [Ruminococcus] torques group

[Ruminococcus] gnavus group

Relative abundance(%)

Age (months)

1298

Figure 4.

1301 **Figure 5.**

1302